





# Driving Galactic Outflows with Magnetic Fields at Low and High Redshift

Ulrich P. Steinwandel<sup>1,2,3</sup> , Klaus Dolag<sup>2,3</sup>, Harald Lesch<sup>2</sup>, and Andreas Burkert<sup>2,4</sup> <sup>1</sup> Center for Computational Astrophysics, Flatiron Institute, 162 5th Avenue, New York, NY 10010, USA; [usteinwandel@flatironinstitute.org](mailto:usteinwandel@flatironinstitute.org)<sup>2</sup> University Observatory Munich, Scheinerstr. 1, D-81679 Munich, Germany<sup>3</sup> Max Planck Institute for Astrophysics, Karl-Scharzschildstr. 1, D-85748, Garching, Germany<sup>4</sup> Max Planck Institute for Extraterrestrial Physics, Giessenbachstr. 1, D-85748, Garching, Germany

Received 2020 December 23; revised 2021 September 22; accepted 2021 October 13; published 2022 January 6

## Abstract

Although galactic outflows play a key role in our understanding of the evolution of galaxies, the exact mechanism by which galactic outflows are driven is still far from being understood and, therefore, our understanding of associated feedback mechanisms that control the evolution of galaxies is still plagued by many enigmas. In this work, we present a simple toy model that can provide insight on how non-axisymmetric instabilities in galaxies (bars, spiral arms, warps) can lead to local exponential magnetic field growth by radial flows beyond the equipartition value by at least two orders of magnitude on a timescale of a few 100 Myr. Our predictions show that the process can lead to galactic outflows in barred spiral galaxies with a mass-loading factor  $\eta \approx 0.1$ , in agreement with our numerical simulations. Moreover, our outflow mechanism could contribute to an understanding of the large fraction of barred spiral galaxies that show signs of galactic outflows in the CHANG-ES survey. Extending our model shows the importance of such processes in high-redshift galaxies by assuming equipartition between magnetic energy and turbulent energy. Simple estimates for the star formation rate in our model together with cross correlated masses from the star-forming main sequence at redshifts  $z \sim 2$  allow us to estimate the outflow rate and mass-loading factors by non-axisymmetric instabilities and a subsequent radial inflow dynamo, giving mass-loading factors of  $\eta \approx 0.1$  for galaxies in the range of  $M_* = 10^9 - 10^{12} M_\odot$ , in good agreement with recent results of SINFONI and KMOS<sup>3D</sup>.

*Unified Astronomy Thesaurus concepts:* Barred spiral galaxies (136); Magnetohydrodynamical simulations (1966); Galaxy winds (626); Magnetic fields (994); Galaxy magnetic fields (604); Milky Way magnetic fields (1057)

## 1. Introduction

Observations in the radio continuum usually indicate a radially declining magnetic field at around  $10 \mu\text{G}$ , observed in a wide range of local spiral galaxies. Locally, the ordered and the turbulent components show different scaling between spiral- and inter-arm regions, where the ordered magnetic field is observed to be higher in the inter-arm regions compared to the spiral arms (e.g., Beck 2015, and references therein). Furthermore, recent observations indicate that many of these galaxies show signs of galactic outflows (e.g., Krause et al. 2018, 2020; Miskolczi et al. 2019; Mora-Partiarroyo et al. 2019; Schmidt et al. 2019; Stein et al. 2019). On top of that there is reported H $\alpha$  emission from nearby galaxies (Vargas et al. 2019) in magnetically active edge-on galaxies, further indicating non-star-forming gas.

Therefore, observationally, it is well constrained that a lot of local magnetized spiral galaxies appear to be quite active in terms of their outflow activity. We suggest that the presence of the magnetic field can self-consistently launch these outflows and account for the observed X-shaped structure in the halo field (Golla & Hummel 1994; Tüllmann & Dettmar 2000; Krause et al. 2006; Heesen et al. 2009; Soida et al. 2011; Stein et al. 2019) due to a wind that is launched by the magnetic pressure. On top of self-consistently generating the observed field structure, such a magnetic-driven process can also directly account for the observed strong fields in the halos of galaxies of

around  $10^{-7}$  G that would then be amplified in the galactic disk due to dynamo action and transported to the halo by the magnetic wind. The process that we suggest consists of the following steps to launch the outflow:

- i. Amplifying the field to equipartition strength via the small-scale turbulent dynamo.
- ii. Ordering the field with the  $\alpha$ - $\Omega$  dynamo on large scales.
- iii. Generating a super-equipartition regime with a low plasma beta by radial inflows due to gravitational instabilities of the galactic disk.
- iv. Generating an open-field geometry to launch the outflow.

Observational studies suggest that  $\sim \mu\text{G}$  magnetic fields in galaxies are in agreement with large-scale dynamo action ( $\alpha$ - $\Omega$  dynamo) in the galactic disk. This argumentation suggests that the large-scale dynamo amplifies a weak magnetic-seed field up to the equipartition (a few  $\mu\text{G}$ ) by small-scale vertical motion of buoyant (supernova) heated bubbles that are lifted up and get sheared by the Coriolis force ( $\alpha$  effect). In rotating spiral galaxies, the magnetic field lines are then supposedly twisted and folded by the large-scale rotation of the disk ( $\Omega$ -effect). While this picture of the large-scale dynamo is a good model to explain the magnetic-field structure in an already evolved spiral galaxy, it represents an oversimplification of how magnetic fields are amplified in the universe.

First, the amplification timescale of the  $\alpha$ - $\Omega$  dynamo in combination with the tiny primordial seed fields in order of  $10^{-20}$  G (e.g., Biermann 1950; Harrison 1970) cannot explain the observed  $\mu\text{G}$  fields today even if one assumes that the Milky Way (MW) formed 13.8 Gyr ago as a fully developed disk, which is in strong disagreement with the findings of

large-volume simulations of the universe (e.g., Teklu et al. 2015; DeFelippis et al. 2017; Lagos et al. 2017; Zjupa & Springel 2017). In addition, observations indicate that galaxies already have very strong magnetic fields at high redshift that are at least as high as the magnetic field today (Perry et al. 1993; Bernet et al. 2008; Kronberg et al. 2008; Wolfe et al. 2008) which furthermore strengthens the timescale argument (see discussion in Section 2.2).

Second, the galactic magnetic field is observed to have a quadrupolar structure. Theoretical models for the  $\alpha$ - $\Omega$  dynamo favor the growth of the dipole mode (see discussion in Section 2.2) and thus the  $\alpha$ - $\Omega$  dynamo as the main amplification process is in tension with the observed field structure. Third, the theoretical model for the  $\alpha$ - $\Omega$  dynamo has boundary conditions that would lead to an excess flux, inconsistent with observed outflow rates in galaxies (see discussion in Section 2.2).

However, from the theoretical point of view this can beautifully be resolved by considering the small-scale turbulent dynamo (e.g., Kraichnan & Nagarajan 1967; Kazantsev 1968; Zeldovich 1983; Kazantsev et al. 1985; Kulsrud & Anderson 1992; Kulsrud et al. 1997; Xu & Lazarian 2020) which amplifies magnetic fields due to stretching, twisting, and subsequent folding of field lines by turbulence driven in the interstellar medium (ISM). This can either happen due to large-scale accretion flows or stellar feedback shown in various numerical simulations (e.g., Beck et al. 2012; Pakmor & Springel 2013; Rieder & Teyssier 2016, 2017a, 2017b; Butsky et al. 2017; Pakmor et al. 2017; Martin-Alvarez et al. 2018, 2020; Hopkins et al. 2020; Steinwandel et al. 2019, 2020a; Su et al. 2018). This dynamo operates on timescales of a few 10 Myr and can quickly amplify a weak primordial seed field at the highest redshifts. Hereby, small-scale turbulence is the main driver of magnetic-field amplification in the ISM and removes the constraint of any ordered large-scale motions of disk galaxies at high redshift. This is in complete agreement with the recent results of galaxy scale simulations and cosmological zoom-in simulations of MW-like galaxies (see Section 3 for a detailed discussion). In this scenario the purpose of the  $\alpha$ - $\Omega$  dynamo is to retain the field once the small-scale turbulent dynamo has generated it, before the field vanishes due to magnetic dissipation.

Furthermore, a magnetic field, established in this fashion contributes massively to the energy density and could potentially trigger a large-scale outflow in a galaxy if there is a mechanism that can efficiently amplify the magnetic field beyond the equipartition field strength. In the following, we will show that this can be achieved by bar formation and radial inflows that will drive the amplification of the field, while the Parker instability provides the field geometry necessary for outflow launching. We therefore suggest that the problem of magnetic-field amplification and the cause for galactic outflows are highly connected problems as the magnetic field can contribute a significant amount to the midplane pressure in the ISM.

In the following we will develop a framework that will explain the formation of a magnetic-driven outflows due to a fast-track dynamo caused by a non-axisymmetric perturbation (bar, spiral arm, warp) in the galactic disk based on the assumption that the small-scale turbulent dynamo amplified the magnetic field beforehand to equipartition field strength and the  $\alpha$ - $\Omega$  dynamo generates the large-scale field structure. Therefore, we first discuss magnetic-field amplification in a galactic context in Section 2 and show how non-axisymmetric instabilities can exponentially amplify the magnetic-field

strength and predict the outflow rate based on magneto-centrifugal wind theory. In Section 3 we show that these simple estimates are consistent with results that can be obtained with numerical simulations at  $z \sim 0$ . In Section 4 we explain how our derived model can impact galactic outflows at  $z \sim 2$ . In Section 5 we summarize our results.

## 2. Theory of Magnetic-field Amplification

### 2.1. Magnetic-seed Fields

Generally, it is assumed that magnetic fields originate from tiny seed fields that arise in the early universe. In the following, we will briefly summarize the various processes for seed-field generation.

The Biermann battery (Biermann 1950) is the most popular process to generate primordial magnetic seeds. It is initiated by nonlinear terms in Ohm's law which lead to a source term in the induction equation that is proportional to  $\nabla p \times \nabla \rho$ . Thus, a tiny magnetic field is induced when the gradients of pressure and density are mis-aligned. This yields a seed field well below  $10^{-21}$  G. However, ionization fronts during the epoch of reionization (EoR, e.g., Spergel et al. 2007) could lead to a more efficient Biermann battery process that sets an upper limit of  $10^{-17}$  (e.g., Gnedin et al. 2000). Harrison (1970) argues that the rotating motion in a sphere of plasma is decoupled from the radiation field at high redshift, due to the increased photon mass at that time. Due to Thompson scattering with the photons, the electrons slow down and induce a current. This induces a magnetic field. As this magnetic-seed field increases, it induces an electric field that stabilizes the rotation of the electrons in the gas sphere. A similar mechanism is proposed by Matarrese et al. (2005). Both mechanisms result in a seed field way below  $10^{-20}$  G. Demozzi et al. (2009) point out that a tiny seed field of the order of  $10^{-32}$  could be generated on Mpc scales during inflation.

However, there are other mechanisms suggested to generate even higher magnetic-seed fields, for example, by the seeding of supernovae. Seeding the magnetic field by supernovae could generate a background field of up to  $10^{-9}$  G in the Galaxy following the studies of Rees (1987, 1994, 2005, 2006). The idea behind this approach is that the magnetic field is generated during stellar evolution (e.g., due to an  $\alpha$ - $\Omega$ -dynamo) and is distributed to the ISM when the star ends its life in a supernova. This can be used to estimate the magnetic-field strength released over the galactic lifetime of roughly 10 Gyr<sup>5</sup> following Beck et al. (2012) who estimate  $10^{-9}$  G Gyr<sup>-1</sup> for a total supernova rate of  $10^8$  within the volume of the Milky Way which is roughly  $300 \text{ kpc}^3$ .

Finally, some authors argue that one can generate a very strong sub-equipartition field of around  $10^{-7}$  G due to plasma instabilities like the Weibel instability (e.g., Schlickeiser & Shukla 2003; Lazar et al. 2009). This is a very intriguing picture because it basically solves the magnetic-seed problem alongside the amplification problem by providing seeds that are just one order of magnitude below the equipartition value of the magnetic field in nearby galaxies. However, Schlickeiser & Shukla (2003) point out that growth only occurs for very high Mach numbers with  $\mathcal{M} > 43$ . Galaxy-cluster simulations (e.g., Miniati et al. 2001; Vazza et al. 2011) from various groups show that there are very few shocks with  $\mathcal{M} > 43$  and almost

<sup>5</sup> This refers to the lifetime of the Galaxy as a fully developed disk.

none with  $\mathcal{M} > 70$  as pointed out by Schlickeiser & Shukla (2003). In combination with the fact that the Weibel instability amplifies the magnetic field on very small scales, this raises the question of whether the instability can generate a coherent high background field on kpc or even Mpc scales.

## 2.2. Amplification due to the $\alpha$ - $\Omega$ Dynamo

Larmor (1919) pointed out that strong magnetic fields could be obtained in a dynamo process in stellar bodies and first attempts for cosmic magnetic-field amplification were made considering axisymmetric velocities by splitting the field in its poloidal and toroidal components. It is straightforward to see that toroidal fields can be generated from poloidal fields by differential rotation (e.g., Kulsrud 2005). This can be understood by considering an initial poloidal field in a differentially rotating disk. The poloidal field lines will move with different velocities in the differentially rotating frame of a galactic disk and some toroidal fields will be generated. Vice versa, if one starts from a purely toroidal field, rotating the disk will only keep the symmetry of the system and there is no amplification of the poloidal component. Thus, rotation alone will not amplify the magnetic field as it will only convert a poloidal field component to a toroidal field component. Therefore, it is impossible to amplify a weak axisymmetric magnetic field by pure axisymmetric motions<sup>6</sup> (see Cowling 1933) to a substantial field strength.

Parker (1955) pointed out that one could generate a significant poloidal field from an initial toroidal field by introducing rising convection cells<sup>7</sup> that are twisted by the Coriolis force of a rotating body when combined with differential rotation. The distortion of the poloidal component would inflict growth in the toroidal component and one obtains exponential growth of the form  $e^{\gamma t}$ . The Parker (1955) dynamo model can be generalized in a mean-field dynamo approximation (Steenbeck et al. 1966) where turbulent motions are treated by the kinetic helicity, quantified by  $\alpha = -\tau/3 \langle \mathbf{v} \cdot \nabla \times \mathbf{v} \rangle$ . Their mixing can be quantified with the turbulent resistivity  $\beta = \tau/2 \langle \mathbf{v} \cdot \mathbf{v} \rangle$ . Introducing fluctuations of velocity and magnetic field of the form  $\mathbf{w} = \mathbf{w}^0 + \mathbf{w}'$ , where  $\mathbf{w}$  is an arbitrary vector quantity. This yields the dynamo equation in thin-disk approximation in cylindrical coordinates:

$$\frac{\partial B_r}{\partial t} = -\frac{\partial}{\partial z}(\alpha B_\phi) + \beta \frac{\partial^2 B_r}{\partial z^2}, \quad (1)$$

$$\frac{\partial B_\phi}{\partial t} = -\Omega B_r + \beta \frac{\partial^2 B_\phi}{\partial z^2}. \quad (2)$$

This can be solved as an Eigenvalue problem with boundary conditions of a thin disk with scale height  $h$  where  $B_r$  and  $B_\phi$  vanish at  $\pm h$  (only valid if  $\beta$  is large) in reduced coordinates, yielding:

$$\gamma' B_r' = -\frac{\partial(z' B_\phi')}{\partial z'} + \frac{\partial^2 B_r'}{\partial z'^2}, \quad (3)$$

<sup>6</sup> If this would be valid, this would correspond to purely linear growth and one can easily show that one would need order of  $10^{14}$  rotations of the MW to reach this field strength while it could have rotated 50 times even if it formed with today's properties at redshift 20.

<sup>7</sup> In disk galaxies rising convection cells could be interpreted as supernova remnants that experience backward motion due to the Coriolis force.

$$\gamma' B_\phi' = D B_r' + \frac{\partial^2 B_\phi'}{\partial z'^2}, \quad (4)$$

with  $z' = z/h$ ,  $t' = \beta t/h^2$ ,  $\gamma' = \gamma h^2/\beta$ ,  $B_\phi = B_\phi'(\beta/h\alpha_0)$ ,  $B_r = B_r'(\beta/h\alpha_0)$ ,  $\alpha_0 = \alpha h/z$  and the dimensionless dynamo number  $D = -\Omega\alpha_0 h^3/\beta^2$ . The solution shows exponential growth for  $D < D_{\text{crit}}$  where  $D^{\text{crit}} < -4$  gives rise to dipole modes and  $D^{\text{crit}} < -13$  gives rise to quadrupole modes on the timescale  $h^2/\beta$ . The growth time depends on the disk-scale height  $h$  and the exact value of  $\beta$ .

Parker (1979) and Ruzmaikin et al. (1988) give an estimate of 0.5 Gyr for a turbulent velocity of  $10 \text{ km s}^{-1}$ , a supernova injection radius of 100 pc, and a disk-scale height of 300 pc, which seems to agree with observed values in the MW. On this timescale, one can amplify a field of  $10^{-14} \text{ G}$  to  $10^{-6}$  over the lifetime of the galactic disk of 6 Gyr. However, we already discussed in Section 2.1 that there are good arguments to assume that primordial seed fields are much lower than  $10^{-14} \text{ G}$ . Therefore, the  $\alpha$ - $\Omega$ -dynamo has a timescale problem.

Furthermore, the magnetic-field structure of the Galaxy is observed to be quadrupolar but the  $\alpha$ - $\Omega$ -dynamo favors a dipole structure. Finally, we note that the boundary conditions for the dynamo equations are problematic as well. In ideal MHD, the field is locked to the fluid. To remove magnetic field at the edges, interstellar matter must vanish from the galaxy, which leads to problems in both the enrichment history of the halo and its energetics (see Kulsrud & Zweibel 2008, their chapter 9, for a detailed discussion). However, the large timescale in combination with the reality of small seed fields from cosmology is the biggest problem and it heavily depends on the estimate of  $\beta$ .

We note that this could be resolved with a better approximation for  $\beta$  (e.g., Poezd et al. 1993; Brandenburg et al. 1995) or a modified dynamo model based on super bubbles (e.g., Ferriere 1992a, 1992b, 1993a, 1993b, 1996, 1998; Ferriere & Schmitt 2000).

Furthermore, we note that a seed field generated by local plasma instabilities could generate a higher seed field around  $10^{-7} \text{ G}$  as we pointed out in Section 2.1. However, there is one crucial thing to keep in mind with this picture. While the large-scale dynamo could amplify such a strong seed field over the timescale of a few Gyr to equipartition, it renders the problem that overdense structures have to act as seed for the Weibel instability. While this could generate the magnetic field in galaxy clusters and massive galaxies, this formation scenario remains in question because it can intrinsically not explain the strong intergalactic magnetic fields and the magnetic fields in voids (e.g., Durrer & Neronov 2013). This could be resolved by galactic winds. However, these winds would have to be quite strong to reach higher magnetic-field strengths in voids.

## 2.3. Amplification due to the Small-scale Turbulent Dynamo

It has been pointed out that the magnetic field could be generated during the formation process (Pudritz & Silk 1989; Kulsrud et al. 1997) of galaxies and galaxy clusters due to strong turbulence, driven by shocks in the high-redshift ISM and ICM. These shocks lead to mis-aligned pressure and density gradients and induce a magnetic field. This leads to a magnetic-field growth proportional to the eddy turnover time of the smallest eddies.

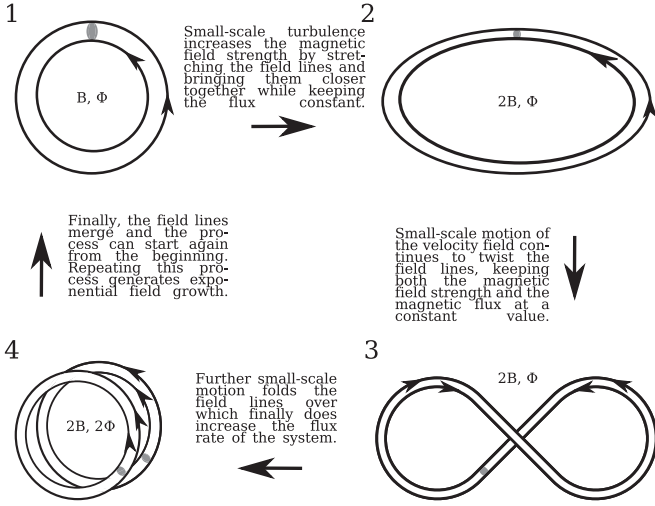


**Figure 1.** Sketch of the stretching twisting and folding of magnetic field lines in the small-scale turbulent dynamo. In this picture, the field strength is increased by stretching a field line at constant magnetic flux. Small-scale turbulent motion then twists and folds the field line which also increases the magnetic flux. Subsequent stretch, twist, and fold events then lead to exponential growth of the field.

This process has been studied extensively in theory (Kraichnan & Nagarajan 1967; Kazantsev 1968; Kulsrud & Anderson 1992; Subramanian & Barrow 2002; Boldyrev & Cattaneo 2004) and is well understood. Mathematically, the idea is to derive the distribution of the power in the magnetic field under the assumption that velocity and magnetic field can be Fourier-decomposed. For random velocities the magnetic power spectrum  $P_M(k)$  is given as the ensemble average of the magnetic energy density:

$$E_{\text{mag}} = \frac{\langle B^2 \rangle}{8\pi} = \int P_M(k) dk. \quad (5)$$

The evolution of  $P_M(k)$  is given as (e.g., Kulsrud & Zweibel 2008):

$$\frac{\partial P_M(k)}{\partial t} = \int K(k, k_0) M(k_0) dk_0 - 2\beta k^2 P_M(k), \quad (6)$$

with the structure function  $K$  and the turbulent resistivity  $\beta$ . Combining Equations (5) and (6) one can find:

$$\frac{dE_{\text{mag}}}{dt} = 2\gamma E_{\text{mag}}, \quad (7)$$

which directly implies that the magnetic-field strength doubles on the timescale of the eddy turnover time. We show this process schematically in Figure 1. The idea is that the field lines are stretched, twisted, and folded by small-scale turbulence. It is worthwhile to note that such a process needs a three-dimensional approach as the folding of the field lines requires an off-plane motion. The growth rate is directly given as the smallest eddy turnover time and the energy is transported via an inverse turbulence cascade to the larger scales. In the kinematic regime, the evolution of  $P_M(k)$  is given via:

$$\frac{\partial P_M(k)}{\partial k} = \frac{\gamma}{5} \left( k^2 \frac{\partial^2 P_M(k)}{\partial k^2} - 2k \frac{\partial P_M(k)}{\partial k} + 6P_M(k) \right) - 2k^2 \lambda_{\text{res}} P_M(k), \quad (8)$$

with the resistivity  $\lambda_{\text{res}}$ . This can be solved in Fourier space and one obtains:

$$P_M(k, t) \propto e^{3/4\gamma t} k^{3/2}, \quad (9)$$

yielding exponential growth of Kazantsev modes with  $k^{3/2}$ . Easy estimates show that this dynamo has eddy turnover times that are smaller by a factor of 100 compared to the freefall time of the proto-galactic halo. While this can easily lead to field strengths that are larger by a factor of 1000 compared to observed fields in today's spiral galaxies, the dynamo saturates when equipartition of the magnetic energy and the turbulent velocity of the smallest eddy is reached. In this picture, one only needs the  $\alpha$ - $\Omega$ -dynamo at low redshift to explain the large-scale correlation of the field and the field is mainly amplified via the small-scale turbulent dynamo. This results in a so-called  $\alpha^2$ - $\Omega$ -dynamo that can generate observed fields in strength and structure.

#### 2.4. How to Locally Generate a Super-equipartition Field

There is some consensus in the literature that magnetic fields are amplified via such a process. The beauty of this is that the fast small-scale turbulent dynamo can quickly amplify the magnetic field, while the large-scale dynamo can order and retain it against magnetic diffusion, for example, due to reconnection events. However, there is an intrinsic problem with driving outflows based on the magnetic field in galaxies. First, magnetic fields are observed to be of the order of a few  $\mu\text{G}$ , which typically corresponds to some equipartition value with cosmic rays and often with the thermal pressure component as well. Driving an outflow via one of the non-thermal components becomes possible if it dominates the thermal component. In other words, for the magnetic field, the following condition has to be valid:

$$\beta = \frac{P_{\text{th}}}{P_B} = \frac{8\pi\rho k_B T}{B^2} \leq 1.0 \quad (10)$$

where  $\beta$  is the plasma parameter, based on the thermal pressure  $P_{\text{th}}$  and the magnetic pressure  $P_B$  of the fluid. At equipartition field strength, this is not the case and the fluid settles at some low value of  $\beta$  that is larger than one. However, to drive an outflow,  $\beta$  needs to be significantly smaller than one. Therefore, the first condition that is needed to drive an outflow via magnetic fields is to generate a super-equipartition field strength. We propose that this super-equipartition regime can be established by non-axisymmetric instabilities like bars, spiral arms, or warps in galactic disks. Every non-axisymmetric instability transports mass inward and angular momentum outward. In the specific case of a bar, this leads to a gas response that is quicker than the outside co-rotation of the bar-like mode with a rotation frequency of the bar  $\Omega_p$  equal to the rotation frequency of the galaxy  $\Omega_g$ .

These processes are quite complicated in nature as they combine rather complex orbital mechanics with the fundamentals of galactic dynamo theory. Therefore, we will discuss the fundamentals of both subjects before we aim to combine them to derive an analytic upper limit for the toroidal field growth induced by gravitational torques.

### 2.4.1. Orbital Dynamics for Spiral Potentials

We will not provide a detailed review on orbital dynamics in spiral potentials but rather introduce the terminology that is needed in order to understand how spiral potentials can alter orbits. An in depth derivation and discussion of the topic is beyond the scope of this paper, but we refer the interested reader to the excellent description in Binney & Tremaine (1987). We follow the description of Binney & Tremaine (1987) and assume that the bar is at rest with respect to a rotating reference frame with initial orientation along the  $x$ -axis. One can then describe the tracer particle orbits by an effective potential that consists of the gravitational potential  $\Phi_0$  of the system corrected for the kinetic energy contribution provided by the pattern speed  $\Omega_p$  of the bar (see also Chiba & Lesch 1994). One finds:

$$\Phi_{\text{eff}} = \Phi_0 - \frac{1}{2}\Omega_p^2(x^2 + y^2). \quad (11)$$

One can solve for the orbits of such a potential with standard Fourier methods. When doing so, one will find that the orbital structure obtained by such a potential can be subdivided into different classes depending on which rotational regime a test particle is located in with respect to the pattern speed  $\Omega_p$ . The most common solution that occurs is denoted as co-rotation with the bar, where the pattern speed  $\Omega_p$  is equal to the orbital speed  $\Omega_0$ . These orbits are reduced to trivial circular orbits when the bar amplitude is vanishing. Once a test particle reaches the regime of inner Lindblad resonance with

$$\Omega_p = \Omega_0 - \frac{\kappa}{2}, \quad (12)$$

with the epicycle-frequency  $\kappa$ , one will find two additional classes of solutions related to the effective potential out of Equation (11). These classes of solutions infer motion alongside the bar potential. One can use the analytic description derived by Binney & Tremaine (1987) for a small-amplitude bar using linear perturbation theory with a perturbing potential given via:

$$\Phi_1 = \Phi_{\text{bar}}(r)\cos 2\varphi, \quad (13)$$

which introduces orbits of the form:

$$r_1(\varphi_0) = A_1 \cos\left(\frac{\kappa\varphi}{\Omega_0 - \Omega_p}\right) + A_2 \cos 2\varphi, \quad (14)$$

where  $\varphi = (\Omega_0 - \Omega_p)t$ . The sign of  $\Omega_0$  denotes the orientation of the orbit of a test particle in the rotating reference frame. While  $A_1$  is an arbitrary (but small) constant,  $A_2$  has a distinct form given via:

$$A_2 = \frac{-1}{\kappa^2 - 4(\Omega_0 - \Omega_p)^2} \left( \frac{d\Phi_{\text{bar}}}{dr} + \frac{2\Omega_0\Phi_{\text{bar}}}{r(\Omega_0 - \Omega_p)} \right). \quad (15)$$

Now, let us assume  $A_1 = 0$  and investigate what happens if  $A_2$  flips its sign. First, one can directly see that we obtain closed orbits with period  $\pi$  if  $A_1 = 0$ . Now there are two possibilities for the orbit alignment depending on the sign of  $A_2$ . On the one hand, if  $A_2 < 0$ , the orbit is perpendicular to the bar. On the other hand, if  $A_2 > 0$ , then the orbit is aligned with the bar.

However, this orbit analysis operates under the assumption that the perturbation is explicitly axisymmetric, but this is an

oversimplification and we will see that the picture becomes more complicated when the perturbation is truly non-axisymmetric.

### 2.4.2. Gravitational Torque by Non-axisymmetric Perturbations

It has been pointed out quite early on by Ostriker & Peebles (1973) that if

$$\frac{T_{\text{rot}}}{|W|} > 0.14, \quad (16)$$

the system is bar-unstable to the mode  $m = 2$ , where  $T_{\text{rot}}$  is the kinetic energy stored in the rotational motion, while  $W$  is the potential energy of the system. This implies that the system is driven into a state in which it is governed by the presence of non-axisymmetric motions. The exact origin of these instabilities has been studied in great detail in Lynden-Bell & Kalnajs (1972) who investigated the evolution of galactic angular-momentum distributions and found that angular momentum is re-shuffled such that particles on low angular velocity orbits gain angular momentum, decreasing the energetic state of the system. Essentially, Lynden-Bell & Kalnajs (1972) showed that gravitational torques can lead to a state of lower angular momentum that results in trailing spiral structure of the system. In this picture, the bar-formation process is then related to trailing modes that are moving through the center which converts them into a leading spiral mode. This mode is then swing-amplified (e.g., Toomre 1981) and converted back into a trailing mode that transports angular momentum outward. However, if angular momentum is transported outward, mass is transported inward and thus bars should be able to effectively feed mass into the central regions of galaxies. This process is leading to a gravitational torque that can be expressed by Larson (1984). The torque that is exhibited by a system with the number  $m$  of spiral arms can be expressed in terms of the wavenumber  $k$  and the radial wavenumber  $k_r$ :

$$J = \frac{m k}{4 k_r} \frac{r\Phi_1^2}{G}, \quad (17)$$

where  $k/k_r$  is the angle  $\alpha$  that describes the offset of a trailing arm with respect to the radial motion in the disk. In first-order perturbation theory, one can express the potential  $\Phi_1 = -(2\pi G/k)\delta\Sigma$ , where  $\delta\Sigma$  denotes the strength of the perturbation. One can re-write Equation (17) to obtain:

$$J = \frac{\pi^2}{m} \sin \alpha \cos^2 \alpha r^3 G (\delta\Sigma)^2. \quad (18)$$

From this, one can derive a timescale for the transport of angular momentum outward and mass inward, triggered by gravitational torques under the assumption of a Keplerian velocity distribution. This timescale  $\tau$  corresponds to the orbital frequency ( $\tau = \partial v_r / \partial r$ )<sup>-1</sup> and we will see in the next chapter that we can initiate magnetic-field growth on a similar timescale for a flow in the radial direction that is initiated by the angular-momentum transfer due to gravitational shearing of the fluid.

### 2.4.3. Simple, Idealized Model for Magnetic-field Amplification in Bars

Under this assumption one can derive an upper limit for the growth of the magnetic field in the toroidal direction by assuming that the flow is oriented alongside the bar and is of low velocity compared to the rotation of the bar by assuming the induction equation for the magnetic-field evolution:

$$\frac{\partial \mathbf{B}}{\partial t} = \nabla \times (\mathbf{v} \times \mathbf{B}) + \eta \Delta \mathbf{B}, \quad (19)$$

we assume  $\eta \approx 0$  to obtain a simple model for azimuthal magnetic-field growth that we solve analytically to get an upper limit for the magnetic-field growth

$$\frac{\partial \mathbf{B}}{\partial t} = \nabla \times (\mathbf{v} \times \mathbf{B}). \quad (20)$$

Furthermore, we assume

$$v_\varphi = r\Omega_0(r). \quad (21)$$

Now we perform a transformation to polar coordinates for the azimuthal component only. This yields

$$\frac{\partial B_\varphi}{\partial t} = -\frac{\partial}{\partial r}(v_r B_\varphi) + B_r r \frac{d\Omega_0}{dr}. \quad (22)$$

We expand the first term on the right-hand side of Equation (22) and find:

$$\frac{\partial B_\varphi}{\partial t} = -B_\varphi \frac{\partial v_r}{\partial r} - v_r \frac{\partial B_\varphi}{\partial r} + B_r r \frac{d\Omega_0}{dr}. \quad (23)$$

Now we move the second term on the right-hand side of Equation (23) to the left-hand side:

$$\frac{\partial B_\varphi}{\partial t} + v_r \frac{\partial B_\varphi}{\partial r} = -B_\varphi \frac{\partial v_r}{\partial r} + B_r r \frac{d\Omega_0}{dr}. \quad (24)$$

Now it is obvious that the term on the left-hand side of Equation (24) marks the substantial derivative that is used to transform between the Eulerian and the Lagrange formulation in hydrodynamics and MHD. Thus, we can re-write Equation (24) in the Lagrange picture in which we advect the fluid along a world line and find

$$\frac{dB_\varphi}{dt} = -\frac{B_\varphi}{\tau} + K, \quad (25)$$

where we introduce  $\tau = -(\partial v_r / \partial r)^{-1}$  and  $K = B_r r \frac{d\Omega_0}{dr}$ . This can be integrated by separating variables which yields

$$B_\varphi = \left[ B_{\varphi,0}(r_0) + \tau B_r r \frac{d\Omega}{dr} \right] e^{t/\tau} - \tau B_r r \frac{d\Omega}{dr}, \quad (26)$$

and we identify  $\tau$  as the amplification timescale. Typically, the timescale of such a process is of the order of 0.1 Gyr (see Lesch 1993; Chiba & Lesch 1994 for details on the timescale estimate). If we now assume that the bar-formation process takes 0.5 Gyr, we obtain magnetic-field growth of the toroidal component by a factor of  $\sim 150$  in the center of the galaxy. If we assume a typical field strength of an already saturated field between 1 and 10  $\mu\text{G}$ , obtained by the  $\alpha^2$ - $\Omega$  dynamo we obtain a central toroidal field between 100 and 1000  $\mu\text{G}$ , which is in accordance with observations of the galactic center (e.g., Yusef-Zadeh et al. 1996). Finally, we note that for a fully

developed bar-like mode, we assume that the magnetic field lines are already perfectly aligned with the bar. This only allows mass flux alongside the radial direction because the mass flux alongside the field lines is force-free in ideal MHD. Thus  $B_r$  remains roughly constant as the bar transports angular momentum outward and mass inward.

Finally, we note that a more detailed derivation of this model is carried out in Section 5 of Chiba & Lesch (1994), who solve for the magnetic-field structure in separate flows which they denote as a flow of closed gaseous orbits (their flow A) and the resulting flow of gas that originates from angular-momentum transport due to the build-up of bars (their flow B). Equation (26) is derived only considering what Chiba & Lesch (1994) denote as flow B. For completeness, we refer the interested reader to Chiba & Lesch (1994) and their very detailed calculation in their Section 5 considering the full picture of flow A and flow B. We close by noting that we want to connect a very easy model for magnetic-field growth to compare to the growth of the field in our simulation in Section 3. We will show that the field growth obtained from our simulation is consistent with the growth rate derived by Chiba & Lesch (1994) for the model from Equation (26) but note that the picture might be much more complex in reality; Equation (26) does not represent the full physics equations but helps us to get a first-order estimate of the field growth (the full picture is treated in Chiba & Lesch 1994, Section 5). Moreover, we note that we need to derive a more detailed analytic model alongside a wider parameter-space exploration in simulations which will be subject of future work but is beyond the scope of this paper.

### 2.5. Driving Outflows with Magnetic Fields

The final goal is now to derive an outflow rate that can be achieved by a magnetic outflow when the fluid has achieved super-equipartition field strength by a factor of 10–100 of the equipartition field in the regime of a few  $\mu\text{G}$ .

We have argued so far that non-axisymmetric perturbations could be responsible for a fast magnetic-field growth. Thus, fast magnetic-field growth could occur in the presence of a strong bar-like mode as observed in many local spirals. However, this does by no means imply that this is the only possibility for fast magnetic-field growth that could result in a super-equipartition state of the field and the following modeling is decoupled from the exact process that drives the field growth but assumes that the findings of our high-resolution multi-physics simulation are somewhat coherent with respect to a certain redshift range in terms of magnetic-field growth and structure alongside the bar. We note that we are aware that this might be a crucial oversimplification. However, developing a more detailed model is beyond the scope of this work as we intend to build an easy understanding of outflow rates based on simple scaling relations.

To determine the outflow rate, we use the concept of magneto-centrifugal wind theory developed by several authors in regimes of stellar winds (Weber & Davis 1967; Mestel 1968), jets (Blandford & Payne 1982), and proto-stellar objects (e.g., Pudritz & Norman 1983; Pelletier & Pudritz 1992; Wardle & Koenigl 1993; Shu et al. 1994; Spruit 1996), which has also been applied to constrain the outflows in starburst galaxies (de Gouveia Dal Pino & Tanco 1999) from a small disk around a central star cluster. The idea is that a collimated wind can be generated by a strong magnetic field in a disk-like configuration

that allows for mass accretion. Typically, it is assumed that the magnetic field in the disk is generated by flux capture of the accreted material.

In our scenario, the magnetic-field growth is triggered by radial flows that enhance growth in the toroidal component. Obviously, in reality, the magnetic-field growth is much more complex than amplification via dynamos or radial flux capture from accreted material. It is most likely a combination of those processes as well as cosmic rays that compete with turbulent diffusion, which will dissipate magnetic fields on the smallest scales.

Furthermore, we assume that the whole central disk of a Milky-Way-like galaxy undergoes gravitational collapse due to the formation of the bar that leads to magnetic-field amplification which will subsequently drive the outflow. Thus, the major difference between the scenario of de Gouveia Dal Pino & Tanco (1999) and ours is that we start from a configuration of a stable disk that undergoes collapse due to non-axisymmetric motions on the scale of roughly 1–2 kpc, while de Gouveia Dal Pino & Tanco (1999) is investigating the outflow on the scale of a few 10–100 pc where a central nuclear disk forms around an active star cluster and the interaction of those two is driving the outflow. We further assume that the baryon overdensity increases toward the centers of galaxies and thus to first order, the same is valid for the energy densities of different components of the ISM as well (e.g., magnetic fields). Spruit et al. (1995) point out that such a configuration can lead to an opening field geometry with  $\beta < 1.0$  which makes this scenario very interesting for our scenario at hand for explaining magnetic-driven outflows in massive spiral galaxies. This is supported by the fact that the gas density right above a galactic disk can be orders of magnitudes lower than the disk material which further reduces  $\beta$  just above the disk.

The field lines anchored in the disk can then support a flow from the disk toward the CGM and collimate it alongside field lines perpendicular to the disk and control the opening angle of the outflow. We suggest that the opening field configuration can be supported by the Parker instability which can generate field lines perpendicular to the disk due to buoyant unstable flows under gravity. Thus, our proposed wind scenario can straightforwardly establish a strongly collimated outflow. This is a fundamental difference between purely starburst-driven winds which are weakly collimated. On top, the proposed scenario can explain the highly magnetized material driven outward in superwinds in nearby galaxies like M82 (e.g., Rich et al. 2010; Roussel et al. 2010; Beirão et al. 2015).

In addition to  $\beta < 1.0$  there are two crucial conditions for outflow launching via the magnetic field: a good coupling between the neutral component and the ions and a high magnetic Reynolds number  $R_m$ . Both are the case as one can carry out a similar estimate as de Gouveia Dal Pino & Tanco (1999) for a disk that is a factor of 10 larger and sits in the center of a Milky-Way-like galaxy, but yields a similar coupling constant between ions and neutral gas in a similarly high magnetic Reynolds number flow. Thus, we have conditions like those presented in de Gouveia Dal Pino & Tanco (1999) and can make a similar estimate for the outflow rate. The key for the success of such a model is a good understanding for the accretion rate toward the galactic center.

The idea behind this is that there is tight coupling between the angular momentum in the central galactic disk and the angular momentum of the wind. This has an interesting

consequence as the wind can then easily remove the angular momentum from the center of the galaxy and support the gravitational collapse of gas toward the galactic center. In classic magneto-centrifugal wind models, one can then find an outflow rate via:

$$\dot{M}_w = f \cdot \dot{M}_a, \quad (27)$$

where  $\dot{M}_w$  is the wind mass-loss rate and  $\dot{M}_a$  is the accretion rate toward the center. The parameter  $f$  describes how much of the accreted mass to the center is coupled to the outflow and scales as  $f = (r/r_A)^2$  where  $r_A$  is the Alfvén radius. The Alfvén radius is the radius in the galactic disk where the magnetic energy density is exceeding the turbulent velocity. We are mainly interested at the value of  $f$  at the driving scale of the wind. Thus, in order to estimate  $f$ , we need to estimate  $r_A$  or directly, the ratio of the driving scale to  $r_A$  as done, for example, in de Gouveia Dal Pino & Tanco (1999), who estimate  $f \approx 0.1$ , which is in good agreement with the general understanding of magneto-centrifugal wind theory.

For now we assume that the driving scale of the wind corresponds to a length-scale of around 250–500 pc and assume that the Alfvén radius is larger by a factor of two to three. Furthermore, we assume that a bar within the Milky Way can transport between 1 and  $2 M_\odot \text{ yr}^{-1}$  toward the galactic center and a star formation rate (SFR) between 0.5 and  $1.0 M_\odot \text{ yr}^{-1}$  in the region of interest due to the mass inflow over the bar. These values are quite moderate and will lead in combination to a factor  $f = 0.1$ , which seems to be in good agreement with other astrophysical systems for which outflow rates have been calculated via magneto-centrifugal wind theory. (e.g., Pelletier & Pudritz 1992).

From this we can obtain an outflow rate by this process in a Milky-Way-like galaxy that corresponds to  $0.05\text{--}0.4 M_\odot \text{ yr}^{-1}$ . Considering the star formation assumed above, this results in low mass-loading factors  $\eta$  with a numerical value of  $\eta$  around 0.1. If such a process would act in the central region of the Milky Way on top of the mass loss due to active galactic nuclei (AGNs) and supernovae, the central region could lose up to  $2 \times 10^8 M_\odot$  over a timescale of 500 Myr. For a galaxy like the Milky Way, this would imply that a fifth of the mass of the central region could be ejected toward the CGM via this process.

We note that the values we assumed so far appear to be quite arbitrary but as we will see in the next section they are in good agreement with the parameters for the Alfvén-radius, the driving scale of the wind and the mass accretion rate over the bar and the SFR in the center of our numerical simulation of a Milky-Way-like galaxy. Moreover, we note that we intrinsically assume that the ratio of the driving scale of such a wind and the Alfvén radius is always constant. This assumption might break down under circumstances where the disk structure is more complicated (e.g., if the disk is strongly warped, the system is tidally stripped, or the system is undergoing a major merger). However, based on the relative similarity of the radial magnetic-field evolution of local spiral galaxies and the fact that our radial magnetic-field profiles (e.g., Beck 2015, for a review) are in rough agreement with these observational trends (Steinwandel et al. 2020a; at least after the dynamo is saturated), this is an acceptable first-order assumption to motivate an easy estimate for the outflow rate based on the magnetic field.

### 3. Evidence from Numerical Simulations and the Situation at $z \sim 0$

Considering numerical simulations, there is evidence on galaxy cluster (e.g., Dolag et al. 2002; Vazza et al. 2018; Roh et al. 2019) and galaxy scales (e.g., Rieder & Teyssier 2016, 2017a, 2017b; Butsky et al. 2017; Pakmor et al. 2017; Martin-Alvarez et al. 2018; Steinwandel et al. 2019) for a small-scale turbulent dynamo that can at least be quantified over the Kazantsev spectrum with a characteristic inverse energy-cascade from small to large scales. For our model we describe the details of the small-scale turbulent dynamo in Steinwandel et al. (2019) and for the large-scale dynamo in Steinwandel et al. (2020a) where we furthermore discuss the role of magnetic fields in driving galaxy outflows based on excess of magnetic pressure over the thermal gas-pressure background of the galaxy. In the following, we will develop a simple toy model that can be used to obtain outflow rates and mass-loading factors by a wind that is initialized by the magnetic pressure alone, informed by our full three-dimensional multi-physics simulation of a Milky-Way-like galaxy.

Analogous to our estimates from Section 2.4 the outflow in our simulation is initialized by the formation of a bar. We show a volume rendering of our simulation of the gas density and the magnetic field in Figure 2 shortly after the formation of the outflow at  $t = 2.233$  Gyr. In Figure 3 we show the bar-formation process in the inner region of the galaxy, which leads to excess mass inflow at the center of the galaxy. However, we note that the mass inflow in the bar is hard to trace as the gas that is transported alongside the bar is of very high density and thus highly star-forming. We quantify this in Figure 4 where we show the mass evolution of the innermost 2 kpc of the galactic disk as a function of time, starting shortly before the accretion process over the bar is initiated (left y-axis, blue lines). From this we can clearly see that the stellar mass of the central region continues to increase, while the gas mass of the central part stays roughly constant. This means that the increase in stellar mass is driven by mass accretion toward the center. The only option for mass accretion to the center in our simulation is from the outer parts of the disk or the CGM, since the simulation is an isolated galaxy. Furthermore, we note that this is consistent with the increase in SFR that we report in the inner region of the galactic disk, shortly after we detect an increase of around 80% of the gas mass of the central part. The SFR increases by roughly the same amount. From the increase of the gas-mass prior to the peak in SFR, we can deduce that the peak inflow rate is around  $1 M_{\odot} \text{ yr}^{-1}$ . This is in accordance with typical mass flow due to angular-momentum transport by a bar. Mass can only flow parallel to the field lines in this configuration. Thus, angular momentum is transported outward and mass inward over the bar. This is the exact setup that we describe in Section 2.4. We note that the central region keeps accreting mass over the bar once the outflow is launched as the outflow can efficiently transport angular momentum out of the center. In the simulation, we find a radial inflow velocity of  $\sim 1 \text{ km s}^{-1}$  which is enough to trigger significant magnetic-field growth in the toroidal direction via Equation (26). We gauge this in Figure 5 where we show the growth of the magnetic field in the innermost 2 kpc of the galaxy which is the region from where the outflow is launched. First, the magnetic field is amplified from a zero-background field via the small-scale turbulent dynamo in the center of the galaxy, which is indicated by the blue line corresponding to the typical eddy turnover time from the small-scale turbulent dynamo in the

ISM. At roughly 1.9 Gyr of evolution of the galactic disk, we find that there is a steep increase of the growth rate by around a factor of four which shortens the characteristic implication time of the magnetic field to 50 Myr. This is faster than typical growth rates of the small-scale turbulent dynamo and is the exact point where we can identify the bar-formation process in Figure 3. Furthermore, the growth rate of this process that we find in the numerical simulations is roughly consistent with the growth rate that we can obtain from Equation (26). As our argument is based on the innermost 2 kpc of our simulation, we need to show that the magnetic field has a physical origin and is not amplified by numerical errors. We discussed this already in depth for the simulation at hand in Steinwandel et al. (2019) where we noted that the numerical divergence is mostly problematic in regions with sharp density gradients, like the transition regions from spiral- to inter-arm regions. Furthermore, we looked into the behavior of the divergence of the central region and can confirm that it is decreasing as a function of time which renders it subdominant for amplification of the magnetic field in our simulation, which we show in Figure 6. We note that the divergence error stays below the percent level for most of the simulation and is actually decreasing for both the mean and the median.

The crucial condition for launching an outflow from any component of the ISM is the pressure dominance of the specific component. Classic feedback processes like stellar feedback in the form of winds, radiation, and supernovae from massive stars launch outflows by increasing the ISM midplane thermal pressure (e.g., Kim & Ostriker 2015; Hu et al. 2016, 2017; Hu 2019; Steinwandel et al. 2020b) and the subsequent formation of super bubbles. In this context, the magnetic pressure has to be of leading order. In other words, the plasma parameter  $\beta = P_{\text{gas}}/P_{\text{B}}$  yields  $\beta < 1.0$ .

In Figure 7 we show the time evolution of the plasma parameter  $\beta$  in the center of the galaxy for four different cuts for the radius between 2 and 0.25 kpc. The galactic center transits from thermal pressure support toward magnetic pressure support, starting at  $t = 1.9$  Gyr with the onset of the bar-formation process in the galaxy, indirectly confirming the strong magnetic-field growth initialized by the bar.

It is interesting to point out that the region between 0.5 and 1.0 kpc is most dominant in establishing  $\beta < 1.0$ . We further note that the outflow is not launched until the innermost region transits to  $\beta < 1.0$ . We show further evidence for this in Figure 8 where we show the radial evolution of  $\beta$  in the innermost 2 kpc for six different points in time. Early into the evolution of the galaxy the center is completely dominated by the thermal gas pressure. Once the bar formation starts, this is quickly changing and the central region is dominated by magnetohydrodynamical behavior rather than hydrodynamical forces.

However, the issue with every outflow process is the coupling of the energy that is stored in the pressure to the ambient medium. In the case of common thermal feedback processes, this happens by thermal gas heating and subsequent thermalization of the hot component to kinetic energy. This question is somewhat more tedious to answer in the case of magneto-centrifugal outflow. In Steinwandel et al. (2020a), we pointed out that there is some evidence that the wind mechanism in the simulation is supported by the Parker instability, which can be identified over the classic Parker-like lobes in the structure of the magnetic-field lines that are lifted



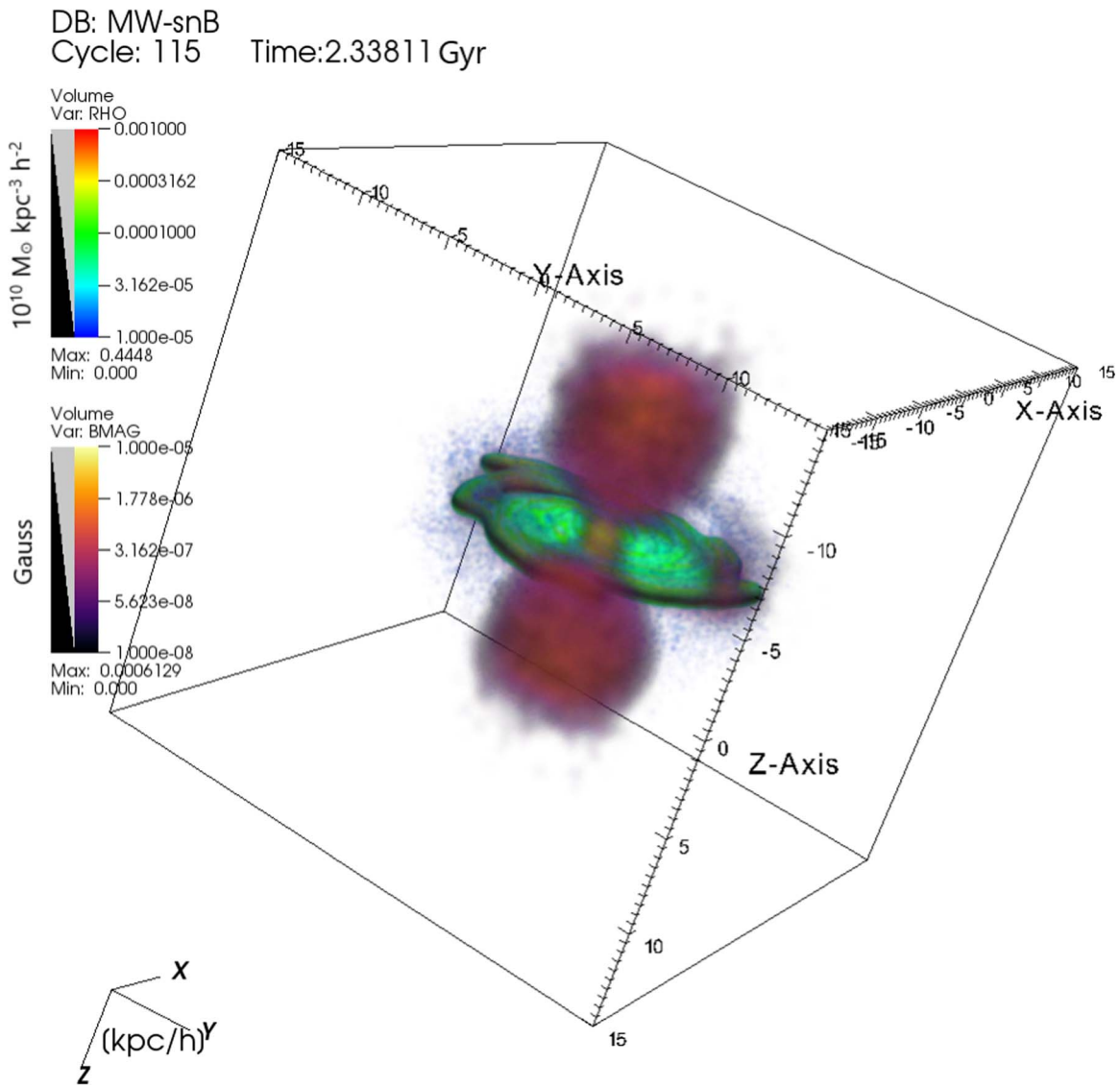


**Figure 2.** We show a 3D volume rendering of the gas density (rainbow colors) and the magnetic-field structure (plasma colors) of our simulated MW analog. We can clearly see the biconal shape of the outflow in the magnetic-field structure. We show the outflow shortly after it has been launched in combination with the bar-formation process, the Parker instability, and adiabatic compression of the magnetic field in the center of the galaxy.

up from the central part of the disk and expand into the lower-density CGM. Thus, the Parker instability could account for the field geometry necessary for launching the outflow.

Moreover, the Parker-like lobes could then directly account for the common X-shaped halo field that is observed in many galaxies that are classified as out-flowing in the CHANG-ES sample of nearby spiral galaxies. If we calculate the outflow rate for our Milky-Way-like model using the prediction of magneto-centrifugal theory, we find outflow rates of the process of the order of  $0.05\text{--}0.4 M_{\odot} \text{ yr}^{-1}$  which is in very good agreement with outflow rates that we find within our simulation that show values around  $0.01\text{--}0.3 M_{\odot} \text{ yr}^{-1}$  resulting in mass-loading factors around 0.1, as can be seen by the magenta point in the bottom left panel of Figure 9 alongside the  $2\sigma$  percentiles on the error bar.

In combination with the results of the CHANG-ES collaboration who report outflow activity and an X-shaped halo field in a lot of the galaxies in their sample. We cross correlated all the galaxies from their sample that could be classified as out-flowing with an X-shaped halo field against their Hubble-type

and find that at least 17 of 22 galaxies<sup>8</sup> of the CHANG-ES galaxies (see Krause et al. 2018, 2020, and references therein) can be classified as barred spiral galaxies. Whether or not our proposed process could play a role for outflows in galaxies could be tested with the upcoming Square Kilometre Array (SKA) in combination with the next generation of IFU surveys that can constrain the kinematic information needed for identifying bars and other non-axisymmetric instabilities.

However, we used a very simple estimate for the ratio of the driving radius of the wind to the Alfvén radius that we obtained from our simulation, which is in accordance with typically derived values for  $f$  around 0.1 for various physical systems (see, for different applications, Pelletier & Pudritz 1992) and we further assumed typical SFRs and inflow rates from our

<sup>8</sup> We specifically refer to the galaxies NGC 891, NGC 2820, NGC 3003, NGC 3044, NGC 3079, NGC 3432, NGC 3556, NGC 3735, NGC 3877, NGC 4013, NGC 4157, NGC 4217, NGC 4302, NGC 4565, NGC 4666, NGC 5775, and UGC 10258. Furthermore, we note that for NGC 4565, the Spitzer Space Telescope revealed a bar in Barentine & Kormendy (2009), but it was classified as a grand-design spiral before.

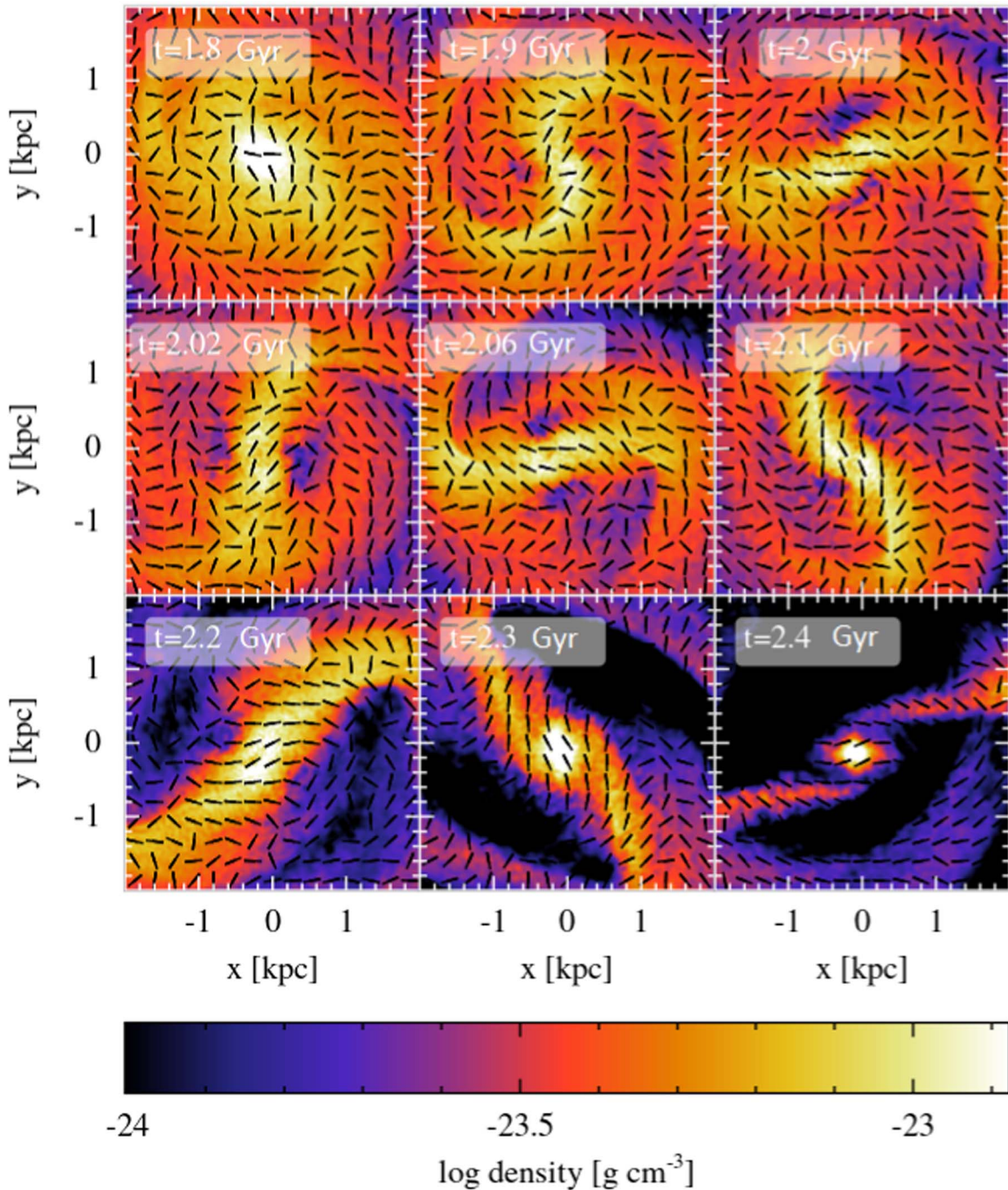


**Figure 3.** Time evolution of the bar-formation process for nine different snapshots. The color shows the projected gas density and the small arrows indicate the direction of the magnetic-field vector. At early times of the bar-formation process we can clearly see that the magnetic-field lines are completely uncorrelated and have no preferred direction. Once the bar is more prominent, we see that the magnetic field aligns with the bar (from  $t = 2$  Gyr). From this moment on, the mass inflow is heavily supported by the bar, as mass can move force-free alongside the magnetic-field lines. Further, this leaves the radial component of the magnetic field roughly constant in the center and the toroidal component is amplified via the radial inflow dynamo which subsequently drives mass flow into the CGM.

simulation using the results of our previous work (Steinwandel et al. 2019, 2020a). Specifically, the model should be improved for directly accounting the additional mass accretion due to the bar on the side of the applied wind model. On the side of the numerical simulation we need better constraints on the driving scale and on the Alfvén radius to develop a more conclusive mode in the future. While our simple estimates should be improved in the future as they only give a first-order estimate of the outflow rate that are motivated by the findings of our

simulation we find good agreement in terms of the mass-loading factor via such a process.

We want to briefly discuss the consequences of such a magnetic-driven outflow for cosmic-ray-driven winds in galaxies. Recently, several groups revived the idea that cosmic rays can significantly contribute to outflows in galaxies (e.g., Hanasz et al. 2013; Girichidis et al. 2016; Pakmor et al. 2016; Pfrommer et al. 2017; Hopkins et al. 2020, 2021a, 2021b, 2021c). This idea is quite intriguing due to the long cooling times of high-energy cosmic rays with respect to the lifetime of galaxies. The general

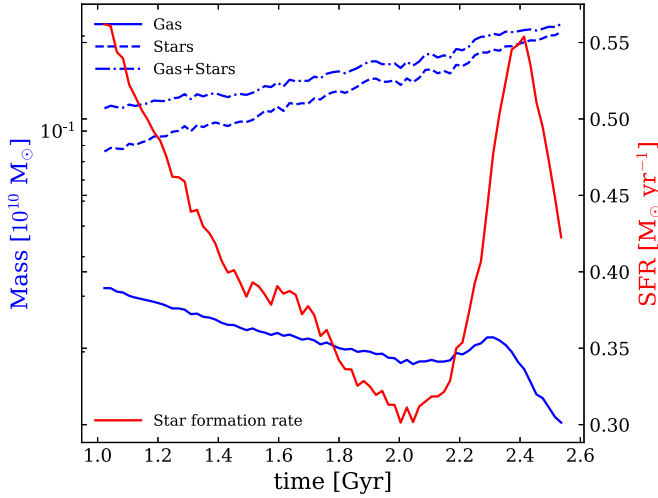


**Figure 4.** We show the mass of the innermost 2 kpc of the galactic disk shortly before the bar-formation process takes place (left y-axis, blue) as well as the star formation rate in this region (right y-axis, red). We see that the central mass in gas and stars is increasing until the magneto-centrifugal outflow sets in. The gas that is funneled toward the innermost kpc by the bar is strongly star-forming and directly converted into stars and the central disk increases its mass mainly over the stellar body (dashed blue line), while the gas reservoir remains more or less constant. However, there is a slight increase in total gas mass that is traced by a peak in star formation shortly after. The slight increase in gas mass is consistent with a peak inflow of around  $1 M_{\odot} \text{ yr}^{-1}$  with a typically lower value that is in accordance with the increase in star formation rate (red solid line) by around 80%.

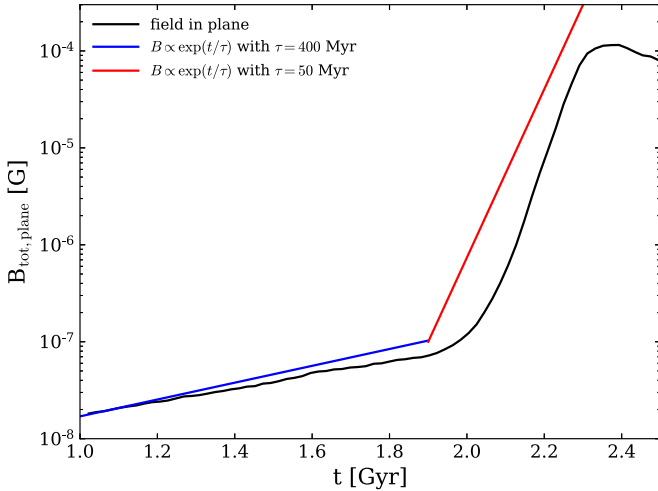


**Figure 5.** We show the magnetic-field growth rate in the innermost 2 kpc of the galaxy within a disk-scale height of 200 pc in the timeframe of 1.0–2.5 Gyr (top). The field grows exponentially until 1.9 Gyr via a small-scale turbulent dynamo with an eddy turnover time of around 400 Myr. After 1.9 Gyr, the dynamo growth rate increases by a factor of 5 and the dynamo grows on a timescale of 50 Myr in the very center. This is faster than the growth rate expected from the small-scale turbulent dynamo alone. The strong increase in the growth rate seems to be correlated with the formation of a bar in the center and the increase of the field strength is roughly consistent with the prediction from the simple radial inflow dynamo. At 2.25 Gyr, the growth is saturated by the large-scale outflow that is driven out of the central region with a low mass-loading factor.

idea of cosmic-ray-driven winds is hereby to generate dominance of the cosmic-ray pressure over the thermal-gas pressure either by cosmic-ray streaming or diffusion. While cosmic-ray streaming generates winds above the midplane, cosmic-ray diffusion can generate a wind at the base of the disk. Hence, diffusion-driven outflows seem to be stronger as they can expel more gas from the

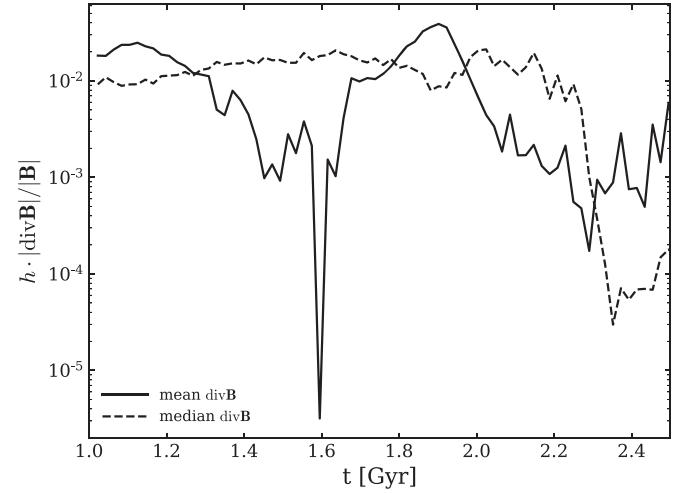


**Figure 6.** We show the evolution of the relative divergence error during the bar-formation process in the innermost 2 kpc of the simulation as the mean (solid) and the median (dashed) lines. Both lines indicate that the divergence error is of the order of 1% in the worst case. We furthermore note that we measure the relative divergence not as an SPH weighted quantity but directly from the particle data, which gives us an upper limit for the divergence error. While the median stays roughly constant during the bar-formation process, the mean is decreasing while the magnetic field is increasing. Thus the magnetic-field growth is not likely to be dominated by spurious amplification of the divergence error. We note that we calculated the divergence error directly from the particle data and not in the SPH stencil. The former typically yields a divergence error that is larger by two to three orders of magnitude. For a more thorough discussion on the computation of the divergence error we refer the reader to Steinwandel et al. (2021).

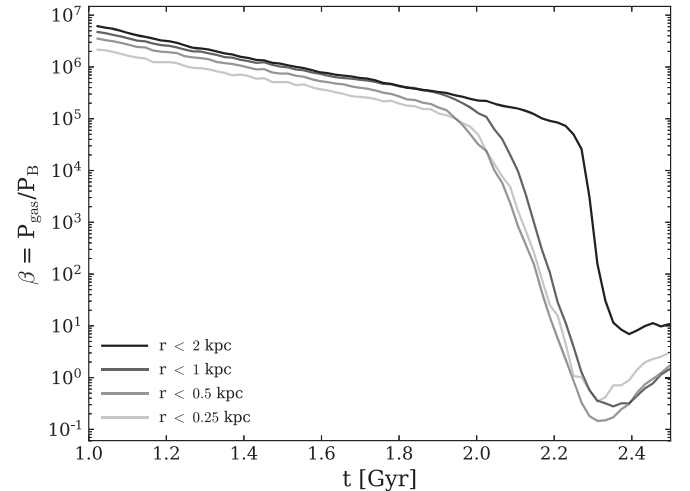


**Figure 7.** We show the plasma  $\beta$  for four different cuts for the innermost radius from 2 kpc to 250 pc. A value of  $\beta > 1$  indicates that the fluid behaves hydrodynamically and is dominated by thermal pressure, while a value smaller than  $\beta < 1$  marks the transition to a fluid that is dominated by the pressure provided by the magnetic field. As the magnetic field is amplified, the center of the galactic disk transits from a state of thermal- to magnetic-dominated. Once the magnetic pressure dominates in the center, the outflow can be launched.

disk. For diffusion-driven winds, this intrinsically depends on the numerical value of the diffusion coefficient that accounts for the coupling. An outflow process as we presented it here could potentially be further enhanced by cosmic-ray-driven winds, which will be the subject of future work. Finally, we note the remarkable resemblance of the structural form of the outflow that we present in Figure 2 with the newly discovered structures above and below the midplane of the Milky Way with EROSITA.

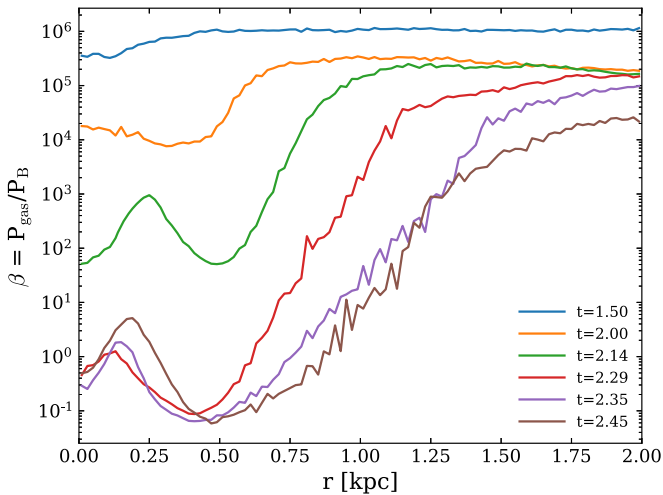


**Figure 8.** We show the radial evolution of the plasma  $\beta$  for six different snapshots close to the outflow-launching process. We see a strong decline of  $\beta$  with time indicating the dominance of the magnetic field in the center of the galaxy shortly before the outflow is triggered. This trend clearly shows that the outflow is subsequently launched because the magnetic field is much stronger than the thermal component.

Predehl et al. (2020) showed that the structures that are typically referred to as the Fermi bubbles extend much further out into the Milky Way halo. Our simulation indicates that a magnetic-driven outflow could form these structures quite efficiently and we think the magnetic field of the Galaxy could play an important role in the formation of these structures alongside the AGN in the galactic center.

#### 4. Consequences for High-redshift Galaxies at $z \sim 2$

Major results from high-redshift observations show that the high-redshift galaxy population is very compact and turbulent with thick disks and has strong galactic outflows and declining gas ratio curves (e.g., Genzel et al. 2014, 2017).

There are some indicators in the line-of-sight velocity profiles (Genzel et al. 2014) that these outflows are driven by the feedback of AGNs or starburst events. However, the line-of-sight velocity profiles indicate structure that allows us to speculate on other outflow mechanisms. We can use our derived outflow process from Section 2.4 and generalize it for the high-redshift population to predict the impact of magnetic outflows in this environment. However, we note that our scenario is completely consistent with that of a starburst-driven outflow where a star cluster is forming in the center of the galaxy, which is surrounded by a disk that keeps accreting mass and increases the magnetic field via flux capture which will generate a low  $\beta$  environment needed for launching the outflow (de Gouveia Dal Pino & Tanco 1999).

On top of this, it is unlikely that in such a regime as the present, at  $z \sim 2$ , magnetic-field amplification takes place via the  $\alpha$ - $\Omega$  dynamo as its timescale increases with  $h^2$  and at  $z \sim 2$ , galaxies show thick disks with declining gas rotation, increasing the turbulent resistivity and decreasing the rotational support, thus suppressing any  $\alpha$ - $\Omega$  dynamo action.

These systems are highly turbulent. The high amount of turbulence in disks at  $z \sim 2$  can start magnetic-field growth via the small-scale turbulent dynamo (kinematic regime) on Myr timescales and the magnetic energy density would quickly establish equipartition with the turbulent energy density,

yielding  $B \propto \sigma_{\text{turb}}$  and increasing the magnetic-field strength in high-redshift systems easily by a factor of 5.

From this, we can directly estimate the SFR of these systems by applying the theoretical scaling of  $B \propto \Sigma_{\text{sfr}}^{1/3}$  that can be obtained analytically following Schleicher & Beck (2013), with the proper redshift correction. A non-axisymmetric instability like a bar but also disk fragmentation (e.g., Behrendt et al. 2015) or cold filament accretion (e.g., Dekel et al. 2009) can now trigger magnetic-field amplification via radial motions. One can cross match the obtained SFRs of our model with the star formation main sequence (MS) at redshift  $z \sim 2$  from which we obtain stellar masses that we can use to calculate the outflow rate by applying the theory of magneto-centrifugal winds and use it in the regime at  $z \sim 2$ .

The latter is the self-consistent way to derive the outflow rate. Therefore, we derive the outflow rate under the assumption that the star formation activity in high-redshift galaxies comes from gas mass that was accreted to the galaxy. We further assume that the driving scale of the outflow is a factor of around three lower than the Alfvén radius of the system, which comes from our redshift zero simulation. This directly implies that  $f = 0.1$  is valid. This is a potential caveat and requires more simulations on our part to improve constraints on driving scales and Alfvén radii as a function of redshift.

Nevertheless, we can use this easy scaling to obtain an outflow rate and, subsequently, the mass loading of a magnetic-driven wind for high-redshift galaxies. This results in values below 1, which is in agreement with the results from Förster Schreiber et al. (2018) for the SINS/ZC-SINF AO survey and from Förster Schreiber et al. (2019) with KMOS<sup>3D</sup>. We show the results for this simple model in Figure 9, where we show the relation between magnetic field and velocity dispersion (top left), our predicted SFRs (top right), outflow rates (bottom left), and mass loadings (bottom right) as a function of stellar mass.

We note that this intrinsically depends on the shape of the star-forming MS at the relevant redshift, which is a clear limitation of the model which we plan to incorporate in future work. Nevertheless, the resulting outflow rates and mass-loading factors are consistent with the theoretical expectations for an energy/entropy-driven outflow and are consistent with the low observed mass-loading factors from Förster Schreiber et al. (2019).

It is interesting to point out an important issue regarding the observed low mass-loading factor in observations and the reality of the high mass-loading factors in numerical simulations, which can reach values above unity even at injection of the underlying feedback model. In cosmological simulations, the mass-loading factor is typically a free parameter to constrain the galaxy population at some target redshift, for example, via the stellar-halo mass relation or the mass-metallicity relation. Therefore, a physical process with low mass loading that can quench star formation and control the mass growth of galaxies is also of potential interest in a cosmological context. However, we are aware of the fact that the mass-loading factor in cosmological simulations is the total mass-loading factor while the one that is constrained from the observations of Förster Schreiber et al. (2019) is connected to the non-star-forming gas as they observe in H $\alpha$ . Therefore, it is potentially possible that there is a lot of mass transport in the cold gas that is simply unaccounted for by current observations, which could justify the higher mass-loading factors in cosmological simulations. In this case, our proposed process

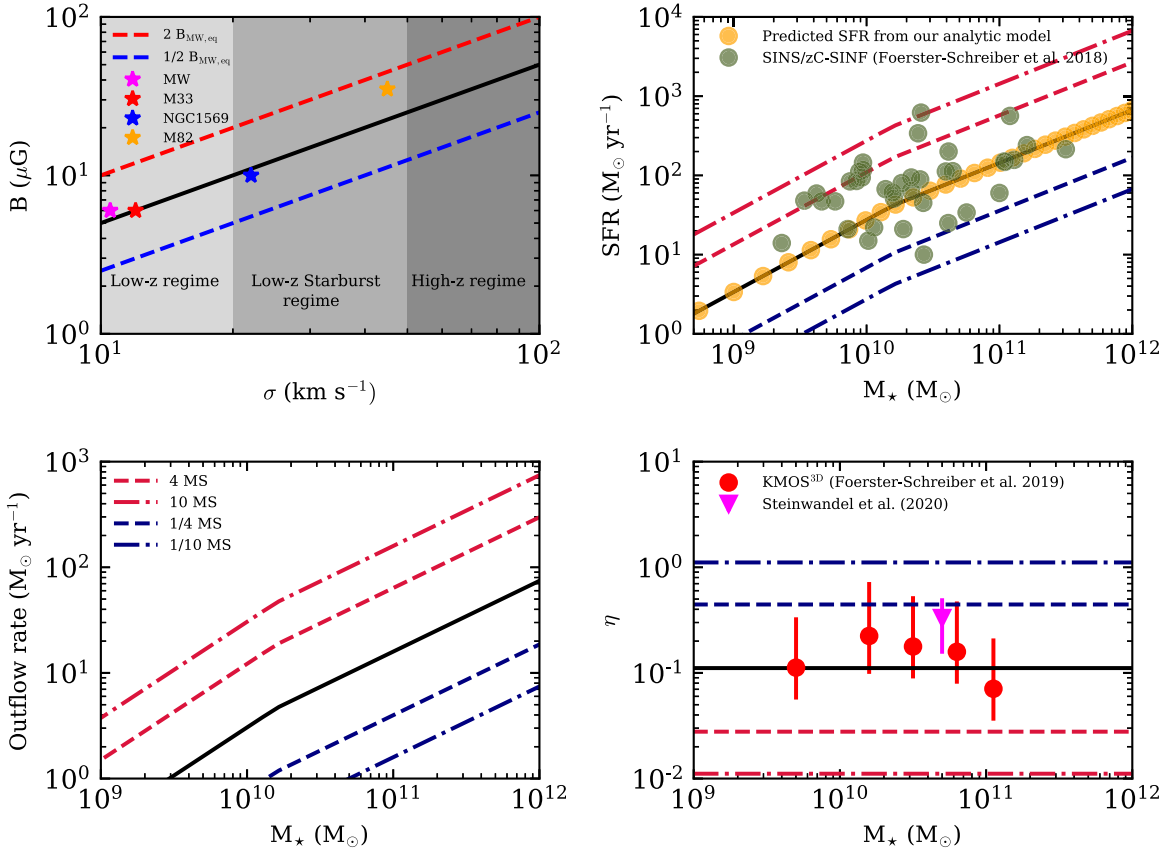


**Figure 9.** This figure shows the main results of our simple toy model prescription for predicting SFRs, outflow rates, and mass-loading factors at  $z \sim 2$ . We assume that the magnetic-field strength in equipartition scales with the turbulent velocity dispersion of the galaxy at hand, which would imply magnetic fields that are of the order of  $30\text{--}50 \mu\text{G}$  in high-redshift galaxies that typically have velocity dispersion of the order of  $40\text{--}120 \text{ km s}^{-1}$  (top left). Moreover, we can compare this to a few galaxies where both the magnetic-field strength and the velocity dispersion can be observed (e.g., in the MW, M33, NGC 1569 and M82). Via the magnetic-field star formation correlation of Schleicher & Beck (2013) we obtain the SFR that corresponds to the higher magnetic-field strength and cross match this against the star formation main sequence at  $z \sim 2$  taken from Whitaker et al. (2014). Finally, we can derive the outflow rate based on the theory of magneto-centrifugal winds. We find a power law increase of the outflow rate with stellar mass (bottom left). Finally, we can obtain the mass-loading factor  $\eta$  by dividing the outflow rate by the SFR (bottom right), which seems to be in good agreement with the mass loading, which is obtained out of our simulation and the observations of the KMOS<sup>3D</sup> instrument. Furthermore, the mass loading by such a magnetic-driven wind appears to be constant which is, for example, different for cosmic-ray-driven winds (e.g., Jacob et al. 2018) and could be used to distinguish between the two processes.

would still contribute to the mass-loading factor in the warm-ionized medium which is extremely important for the baryon cycle of galaxies. We discuss these issues in greater detail in Appendix B. Our predictions could be tested by evaluating the magnetic-field strengths in  $z \sim 2$  galaxies with SKA in combination with high-resolution IFU-spectrographs that can reveal the kinematic structure of these galaxies.

## 5. Conclusions

We discussed the possibility and the consequences of magnetic-driven outflows across redshift. We pointed out that spiral galaxies with a strong magnetic field on the order of a few  $\mu\text{G}$  should be able to drive magnetic outflows with low mass-loading factors if certain conditions are met. First, there must be a process that can amplify the magnetic field to equipartition and provides the observed large-scale field structure. From state-of-the-art numerical simulations there is overwhelming evidence for the small-scale turbulent dynamo as the main amplification process for the steady-state magnetic field. However, the observed magnetic-field structure that is correlated on kpc scales seems to be consistent with the classic picture of the  $\alpha\text{--}\Omega$  dynamo which is assumed to be too slow in amplifying the magnetic field on Gyr timescales to observed

values. Thus we argue for an  $\alpha^2\text{--}\Omega$  dynamo in which the small-scale dynamo is amplifying the field and the large-scale dynamo is ordering and retaining the field against magnetic dissipation.

We showed that a steady-state-field can undergo fast exponential growth via radial flows if the galaxy forms a bar in its evolution. We find that such a process can amplify the field by at least an order of magnitude over the timescale of around 500 Myr, which is enough to generate a plasma beta of around 0.1 which is the perfect environment for launching a galactic wind by magnetic fields. We further assume that the Parker instability is providing the magnetic-field structure needed for launching the outflow. The outflow process that we suggest is driven from the central region of massive spiral galaxies once they become bar-unstable and has a driving scale of a few 100 pc. The outflow rates that we obtain are consistent within the framework of magneto-centrifugal wind theory in terms of the predicted outflow rate and show excellent agreement with our numerical simulation. Furthermore, the proposed structure resembles the structure of the Fermi bubbles which have recently been observed to be much larger than originally expected. Thus, our outflow mechanism could also partially play a role in explaining the new structure above and

below the midplane of the Milky Way as revealed very recently by eRosita (Predehl et al. 2020).

Moreover, the combination of our model predictions and our numerical simulations can directly explain why so many galaxies of the CHANG-ES sample that show a bar also show signs of outflows (e.g., Krause et al. 2018, 2020).

Furthermore, it is possible to extend our modeling to galaxies at  $z \sim 2$ . The model is able to predict the observed SFRs at  $z \sim 2$ . Cross correlating the obtained SFRs with the MS at  $z \sim 2$  yields the observed high outflow rates and low mass-loading factors that are observed with KMOS<sup>3D</sup> in Förster Schreiber et al. (2019) who also find evidence for non-axisymmetric perturbations of the galaxies at  $z \sim 2$  (Förster Schreiber et al. 2019).

We propose that our suggested outflow process can contribute to the baryon budget of galaxies at low and high redshift. We believe that this can be tested with future IFU surveys at high redshift in combination with the capabilities of SKA that will provide us with magnetic-field strength and kinematic information out to large redshifts.

We thank the referee for comments that greatly improved the quality of the paper and helped us to gain a deeper understanding of the complex topic of galactic magnetic fields. U.P.S. is supported by the Simons Foundation through a Flatiron Research Fellowship (FRF) at the Center for Computational Astrophysics. The Flatiron Institute is supported by the Simons Foundation. U.P.S. acknowledges valuable comments by Eirini Batziou, Ludwig Boess, Aura Obreja, and Joseph O’Leary. U.P.S., K.D., H.L., and A.B. acknowledge support from the Deutsche Forschungsgemeinschaft (DFG, German Research Foundation) under Germany’s Excellence Strategy—EXC-2094-390783311 from the DFG Cluster of Excellence “ORIGINS.”

U.P.S. acknowledges funding by the Deutsche Forschungsgemeinschaft (DFG, German Research Foundation) with the project number MO 2979/1-1.

U.P.S. acknowledges computing time granted by the Leibniz Rechenzentrum (LRZ) in Garching under the project number pn72bu and computing time granted by the c2pap-cluster in Garching under project number pr27mi. U.P.S. acknowledges computing time provided by the resources at the Flatiron Institute on the clusters Rusty and Popeye.

### Data Availability Statement

The data is available based on reasonable request to the corresponding author.

## Appendix A

### Radial Inflows and Magnetic Diffusivity

As we already pointed out in Section 2.4, neglecting the diffusion term leads to an upper limit of our modeling. The problem with dropping the diffusion term is two-fold. The first problem that arises is that the diffusion term is needed for a proper dynamo model. However, the idea of this paper is to get an easy analytic insight on how magnetic fields could potentially drive outflows over a wide range of galaxy mass and redshift and not to model the detailed influence of the radial inflow on the dynamo growth rate, which would be a different study. The second problem that arises by dropping the diffusion term is simply that there is no

intrinsic dissipation of magnetic energy on the smallest scales, which leads to an overestimate of the field growth. This has already been pointed out before. Moss et al. (2000) solved the classic dynamo equations under the assumption of an additional radial inflow of the order of  $1 \text{ km s}^{-1}$  while accounting for the diffusion term. Moss et al. (2000) point out that Chiba & Lesch (1994) dropped the diffusion term and they consider this a strong oversimplification of the situation as Chiba & Lesch (1994) draw the conclusion from their result that radial inflows can explain magnetic-field growth in galaxies altogether. While it is true that the model of Chiba & Lesch (1994) is missing the diffusion term, we use this model in this work to get an analytic insight on the growth rate of the magnetic field in the innermost 2 kpc of our MW-like disk-galaxy simulation of which we showed small-scale and large-scale dynamo growth in Steinwandel et al. (2019, 2020a). As Moss et al. (2000) brings forward the strongest criticism of the model of Chiba & Lesch (1994) we want to discuss why the regime that we consider is different from the regime that is discussed in both, Chiba & Lesch (1994) and Moss et al. (2000). The idea for our model is motivated by our simulations. As we showed in Figure 5 from our own simulations, there is evidence for a strong increase of the growth rate of the magnetic field in the plane of the innermost 2 kpc within the disk-scale height of 200 pc. The growth rate of the magnetic field increases by a factor of 5 when the bar-formation process in the center of the galaxy starts. The jump in the growth rate and the bar formation are therefore tightly correlated which is clearly shown by our simulations and is in rough agreement with the predicted growth rate for amplification by Chiba & Lesch (1994) within a factor of 2. Our simulation indicates hereby slightly faster dynamo growth than the model from Chiba & Lesch (1994). In contrast to this, the detailed treatment and solution of the dynamo equations by Moss et al. (2000) indicates that radial flows in barred spiral galaxies could reduce the dynamo growth rate by around 20%–30% which is true for radial flows with positive and negative sign. However, a reduced growth rate of the dynamo and a correlated lower saturation value do not indicate that there is not net growth of the field. Moss et al. (2000) back up their results with a two-dimensional simulation which is much different than our three-dimensional multi-physics simulation that resolves the adiabatic compression regime and the small-scale and the large-scale dynamo, incorporates a treatment for star formation and stellar feedback, and is suited to the investigation of magnetic-field growth from a zero-background field. Furthermore, the focus of Moss et al. (2000) and the argument on suppressed dynamo growth is focused on the conditions in the solar neighborhood, which we do not apply as we strictly consider magnetic-field growth within the innermost 2 kpc as an indication for driving outflows based on the magnetic pressure in local spiral galaxies. Moss et al. (2000) provide us with an estimate for the saturation value of the toroidal magnetic field at the solar radius for a radial flow of  $1 \text{ km s}^{-1}$  and find  $B_\varphi \approx 10 \mu\text{G}$ . However, if we assume more realistic values for our configuration we obtain a value of around  $B_\varphi \approx 100 \mu\text{G}$  for the saturation value which is in good agreement with our predicted saturation field strength from our simulations. This is related to the fact that the correction terms determined by Moss et al. (2000) are scaling with  $R^2$  and  $v_r^2$ , where  $R$  is the distance from the

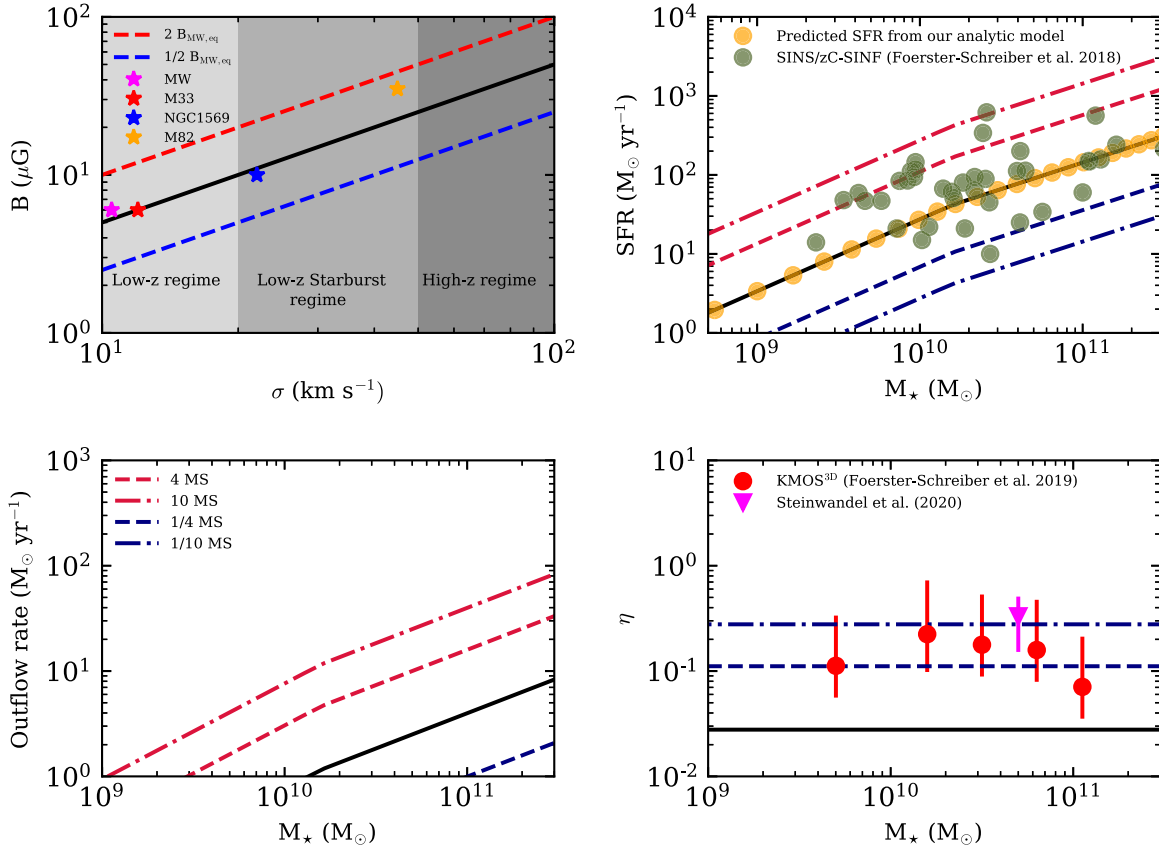


**Figure 10.** Same as Figure 9 but assuming that the magnetic-field growth is suppressed by 30% as pointed out by Moss et al. (2000). However, we note that in our case, the correction term of Moss et al. (2000) is quite small as we are closer to the center and the correction term scales with radius squared.

center of rotation and  $v_r$  is the radial velocity. As the distance from the rotation center is much smaller in our case, we find a weaker deviation from the dynamo growth rate. Furthermore, we note that the situation is much more complicated in our case as we resolve the small-scale turbulent dynamo action. Thus, it could be possible that the amplification is only indirectly triggered by the inflow as star formation in the center increases due to the radial inflow which will increase turbulence and might simply shorten the eddy turnover time that is correlated with the growth rate of the small-scale turbulent dynamo. However, as this amount of turbulence is triggered by the radial inflow, the magnetic-field amplification can then be estimated to first order by increase obtained over the radial inflow and the subsequent amplification of the magnetic field which appears to be consistent with the easy model by Chiba & Lesch (1994). Consideration of the diffusion term would then lead to a slightly lower saturation value in the center which would still be in agreement with the saturation value for the central plane predicted by our simulations. We note that our argument slightly differs from the high-redshift systems as we intrinsically assume that feedback is so strong that those systems constantly become gravitationally unstable in their dark-matter potential. We show modified model predictions by taking a smaller growth rate of the dynamo in the center into account in Figure 10 from which we directly see that the growth rate of the dynamo due to radial inflow is not dominating the mass loading even if radial flows suppress the dynamo action by a 30% margin.

## Appendix B The Interdisciplinary Nature of This Approach

This work has a highly interdisciplinary nature and we want to briefly put our work into the context of the different sub-fields to which it is related. First, the contribution in the area of galactic magnetic fields is apparent by the fact that our simulations show resolved dynamo action from the small-scale dynamo and the large-scale dynamo as we reported in Steinwandel et al. (2019) for the small-scale turbulent dynamo and in Steinwandel et al. (2020a) for the large-scale dynamo. However, we find the leading order in magnetic-field amplification is driven by the small-scale turbulent dynamo. Furthermore, our simulations are not the only ones that predict this outcome (see, e.g., Rieder & Teyssier 2016, 2017a; Pakmor et al. 2017). In our picture, the large-scale dynamo is only needed for ordering the field on the larger scales as the small-scale turbulent dynamo struggles to explain the large correlation lengths of the magnetic field in the Galaxy. However, Rieder & Teyssier (2017a) suggest that the large-scale magnetic-field structure could also be generated by infalling gas from the CGM. Furthermore, there is analytic work from Xu & Lazarian (2020) which could explain the kpc correlation lengths due to the nonlinear growth of the dynamo modes. However, we find that the large-scale dynamo is the leading process for ordering the field on larger scales to a quadrupolar structure that is consistent with observations (Stein et al. 2019).

Second, there is the outflow aspect of this work. Our simulations indicate an outflow with a low mass-loading factor for MW-like spiral galaxies. In this context, we point out the

interesting aspect that observed local spiral galaxies that show a sign of outflows seem to be heavily biased toward being classified as barred spiral galaxies. Often these outflows are explained either by stellar feedback or by the cosmic-ray pressure component that can launch them from the ISM. We ask the simple question: What if these outflows are driven by the magnetic pressure instead of the cosmic-ray pressure due to strong magnetic-field amplification in the central part of massive spiral galaxies that undergo a gravitational instability and drive magnetic-field growth in the center as a combination of adiabatic compression and a fast-dynamo process? Our outflow due to the magnetic-field structure provided by the buoyancy (Parker) instability in the magnetically overpressurized medium is different from classic wind-launching processes in galaxies. Our simplified model can either be confirmed or be out ruled with a combination of upcoming surveys like SKA and the next generation of high-resolution IFUs that can give insight into the detailed gas structure.

Finally, there is the galaxy formation aspect of this work for which we try to evaluate the importance of magnetic fields in massive galaxies at higher redshift and discuss the consequences of gravitational (bar-like) modes and elaborate on whether a strong magnetic field at high redshift could launch an outflow. By doing so, we find that our very simple model that is easy to understand predicts magnetic-driven outflows at higher redshift with low mass loading. Numerical simulations (specifically, large cosmological volumes) typically assume some mass loading, which is much higher than suggested by observations. This is specifically true for the galaxies at the high mass end of the stellar mass function. In large cosmological volumes, the mass-loading  $\eta$  is typically a free parameter of the modeling which is tuned to reproduce some quantity at redshift zero (e.g., the stellar mass function or the mass-metallicity relationship of galaxies). Our simulations suggest a process that can quench star formation by self-consistently establishing a magnetic outflow with very low mass loading in agreement with observations at low redshift. In combination with our simple toy model we can investigate if such a process can establish a similar outflow with low mass loading at higher redshift. Such processes are important to study because they are decoupled from the thermal feedback loop of galaxies and the observed variations in the velocity line profiles of high-redshift galaxies would potentially allow for different feedback channels apart from thermal feedback by supernovae, stellar winds, and AGNs.

### ORCID iDs

Ulrich P. Steinwandel  <https://orcid.org/0000-0001-8867-5026>

Andreas Burkert  <https://orcid.org/0000-0001-6879-9822>

### References

- Barentine, J. C., & Kormendy, J. 2009, in ASP Conf. Ser. 419, *Galaxy Evolution: Emerging Insights and Future Challenges*, ed. S. Jogee et al. (San Francisco, CA: ASP), 149
- Beck, A. M., Lesch, H., Dolag, K., et al. 2012, *MNRAS*, 422, 2152
- Beck, R. 2015, *A&ARv*, 24, 4
- Behrendt, M., Burkert, A., & Schartmann, M. 2015, *MNRAS*, 448, 1007
- Beirão, P., Armus, L., Lehnert, M. D., et al. 2015, *MNRAS*, 451, 2640
- Bernet, M. L., Miniati, F., Lilly, S. J., Kronberg, P. P., & Dessauges-Zavadsky, M. 2008, *Natur*, 454, 302
- Biermann, L. 1950, *ZNatA*, 5, 65
- Binney, J., & Tremaine, S. 1987, *Galactic Dynamics* (Princeton, NJ: Princeton Univ. Press)
- Blandford, R. D., & Payne, D. G. 1982, *MNRAS*, 199, 883
- Boldyrev, S., & Cattaneo, F. 2004, *PhRvL*, 92, 144501
- Brandenburg, A., Moss, D., & Shukurov, A. 1995, *MNRAS*, 276, 651
- Butsky, I., Zrake, J., Kim, J.-H., Yang, H.-I., & Abel, T. 2017, *ApJ*, 843, 113
- Chiba, M., & Lesch, H. 1994, *A&A*, 284, 731
- Cowling, T. G. 1933, *MNRAS*, 94, 39
- DeFelippis, D., Genel, S., Bryan, G. L., & Fall, S. M. 2017, *ApJ*, 841, 16
- de Gouveia Dal Pino, E. M., & Tanco, G. A. M. 1999, *ApJ*, 518, 129
- Dekel, A., Birnboim, Y., Engel, G., et al. 2009, *Natur*, 457, 451
- Demozzi, V., Mukhanov, V., & Rubinstein, H. 2009, *JCAP*, 2009, 025
- Dolag, K., Bartelmann, M., & Lesch, H. 2002, *A&A*, 387, 383
- Durrer, R., & Neronov, A. 2013, *A&ARv*, 21, 62
- Ferriere, K. 1992a, *ApJ*, 391, 188
- Ferriere, K. 1992b, *ApJ*, 389, 286
- Ferriere, K. 1993a, *ApJ*, 409, 248
- Ferriere, K. 1993b, *ApJ*, 404, 162
- Ferriere, K. 1996, *A&A*, 310, 438
- Ferriere, K. 1998, *A&A*, 335, 488
- Ferrière, K., & Schmitt, D. 2000, *A&A*, 358, 125
- Förster Schreiber, N. M., Renzini, A., Mancini, C., et al. 2018, *ApJS*, 238, 21
- Förster Schreiber, N. M., Übler, H., Davies, R. L., et al. 2019, *ApJ*, 875, 21
- Genzel, R., Förster Schreiber, N. M., Rosario, D., et al. 2014, *ApJ*, 796, 7
- Genzel, R., Schreiber, N. M. F., Übler, H., et al. 2017, *Natur*, 543, 397
- Girichidis, P., Naab, T., Walch, S., et al. 2016, *ApJL*, 816, L19
- Gnedin, N. Y., Ferrara, A., & Zweibel, E. G. 2000, *ApJ*, 539, 505
- Golla, G., & Hummel, E. 1994, *A&A*, 284, 777
- Hanasz, M., Lesch, H., Naab, T., et al. 2013, *ApJL*, 777, L38
- Harrison, E. R. 1970, *MNRAS*, 147, 279
- Heesen, V., Beck, R., Krause, M., & Dettmar, R. J. 2009, *A&A*, 494, 563
- Hopkins, P. F., Chan, T. K., Garrison-Kimmel, S., et al. 2020, *MNRAS*, 492, 3465
- Hopkins, P. F., Chan, T. K., Ji, S., et al. 2021a, *MNRAS*, 501, 3640
- Hopkins, P. F., Chan, T. K., Squire, J., et al. 2021b, *MNRAS*, 501, 3663
- Hopkins, P. F., Squire, J., Chan, T. K., et al. 2021c, *MNRAS*, 501, 4184
- Hu, C.-Y. 2019, *MNRAS*, 483, 3363
- Hu, C.-Y., Naab, T., Glover, S. C. O., Walch, S., & Clark, P. C. 2017, *MNRAS*, 471, 2151
- Hu, C.-Y., Naab, T., Walch, S., Glover, S. C. O., & Clark, P. C. 2016, *MNRAS*, 458, 3528
- Jacob, S., Pakmor, R., Simpson, C. M., Springel, V., & Pfrommer, C. 2018, *MNRAS*, 475, 570
- Kazantsev, A. P. 1968, *JETP*, 26, 1031
- Kazantsev, A. P., Ruzmaikin, A. A., & Sokolov, D. D. 1985, *ZhETF*, 88, 487
- Kim, C.-G., & Ostriker, E. C. 2015, *ApJ*, 802, 99
- Kraichnan, R. H., & Nagarajan, S. 1967, *PhFl*, 10, 859
- Krause, M., Irwin, J., Schmidt, P., et al. 2020, *A&A*, 639, A112
- Krause, M., Irwin, J., Wiegert, T., et al. 2018, *A&A*, 611, A72
- Krause, M., Wielebinski, R., & Dumke, M. 2006, *A&A*, 448, 133
- Kronberg, P. P., Bernet, M. L., Miniati, F., et al. 2008, *ApJ*, 676, 70
- Kulsrud, R. M. 2005, *Plasma Physics for Astrophysics* (Princeton, NJ: Princeton Univ. Press)
- Kulsrud, R. M., & Anderson, S. W. 1992, *ApJ*, 396, 606
- Kulsrud, R. M., Cen, R., Ostriker, J. P., & Ryu, D. 1997, *ApJ*, 480, 481
- Kulsrud, R. M., & Zweibel, E. G. 2008, *RPPH*, 71, 046901
- Lagos, C. d. P., Theuns, T., Stevens, A. R. H., et al. 2017, *MNRAS*, 464, 3850
- Larmor, J. 1919, How Could a Rotating body Such as the Sun become a Magnet? (Rep. 87th Meet. Brit. Assoc. Adv. Sci), 87, 159, <https://www.biodiversitylibrary.org/item/96028#page/245/mode/lup>
- Larson, R. B. 1984, *MNRAS*, 206, 197
- Lazar, M., Schlickeiser, R., Wielebinski, R., & Poedts, S. 2009, *ApJ*, 693, 1133
- Lesch, H. 1993, in *IAU Symp. 157, The Cosmic Dynamo*, ed. F. Krause, K. H., & G. Rudiger (Dordrecht: Kluwer), 395
- Lynden-Bell, D., & Kalnajs, A. J. 1972, *MNRAS*, 157, 1
- Martin-Alvarez, S., Devriendt, J., Slyz, A., & Teyssier, R. 2018, *MNRAS*, 479, 3343
- Martin-Alvarez, S., Slyz, A., Devriendt, J., & Gómez-Guijarro, C. 2020, *MNRAS*, 495, 4475
- Matarrese, S., Mollerach, S., Notari, A., & Riotto, A. 2005, *PhRvD*, 71, 043502
- Mestel, L. 1968, *MNRAS*, 138, 359
- Miniati, F., Ryu, D., Kang, H., & Jones, T. W. 2001, *ApJ*, 559, 59
- Miskolczi, A., Heesen, V., Horellou, C., et al. 2019, *A&A*, 622, A9
- Mora-Partiarroyo, S. C., Krause, M., Basu, A., et al. 2019, *A&A*, 632, A11



- Moss, D., Shukurov, A., & Sokoloff, D. 2000, *A&A*, **358**, 1142
- Ostriker, J. P., & Peebles, P. J. E. 1973, *ApJ*, **186**, 467
- Pakmor, R., Gómez, F. A., Grand, R. J. J., et al. 2017, *MNRAS*, **469**, 3185
- Pakmor, R., Pfrommer, C., Simpson, C. M., & Springel, V. 2016, *ApJL*, **824**, L30
- Pakmor, R., & Springel, V. 2013, *MNRAS*, **432**, 176
- Parker, E. N. 1955, *ApJ*, **122**, 293
- Parker, E. N. 1979, *Cosmical Magnetic Fields. Their Origin and their Activity* (Oxford: Clarendon Press)
- Pelletier, G., & Pudritz, R. E. 1992, *ApJ*, **394**, 117
- Perry, J. J., Watson, A. M., & Kronberg, P. P. 1993, *ApJ*, **406**, 407
- Pfrommer, C., Pakmor, R., Schaal, K., Simpson, C. M., & Springel, V. 2017, *MNRAS*, **465**, 4500
- Poezd, A., Shukurov, A., & Sokoloff, D. 1993, *MNRAS*, **264**, 285
- Predehl, P., Sunyaev, R. A., Becker, W., et al. 2020, *Natur*, **588**, 227
- Pudritz, R. E., & Norman, C. A. 1983, *ApJ*, **274**, 677
- Pudritz, R. E., & Silk, J. 1989, *ApJ*, **342**, 650
- Rees, M. J. 1987, *QJRAS*, **28**, 197
- Rees, M. J. 1994, in *NATO ASI Ser., Ser. C*, ed. D. Lynden-Bell, Vol. 422 (Dordrecht: Kluwer), 155
- Rees, M. J. 2005, in *Cosmic Magnetic Fields*, ed. R. Wielebinski & R. Beck, Vol. 664 (Berlin: Springer), 1
- Rees, M. J. 2006, *AN*, **327**, 395
- Rich, J. A., Dopita, M. A., Kewley, L. J., & Rupke, D. S. N. 2010, *ApJ*, **721**, 505
- Rieder, M., & Teyssier, R. 2016, *MNRAS*, **457**, 1722
- Rieder, M., & Teyssier, R. 2017a, *MNRAS*, **471**, 2674
- Rieder, M., & Teyssier, R. 2017b, *MNRAS*, **472**, 4368
- Roh, S., Ryu, D., Kang, H., Ha, S., & Jang, H. 2019, *ApJ*, **883**, 138
- Roussel, H., Wilson, C. D., Vigroux, L., et al. 2010, *A&A*, **518**, L66
- Ruzmaikin, A., Sokolov, D., & Shukurov, A. 1988, *Natur*, **336**, 341
- Schleicher, D. R. G., & Beck, R. 2013, *A&A*, **556**, A142
- Schlickeiser, R., & Shukla, P. K. 2003, *ApJL*, **599**, L57
- Schmidt, P., Krause, M., Heesen, V., et al. 2019, *A&A*, **632**, A12
- Shu, F., Najita, J., Ostriker, E., et al. 1994, *ApJ*, **429**, 781
- Soida, M., Krause, M., Dettmar, R. J., & Urbanik, M. 2011, *A&A*, **531**, A127
- Spergel, D. N., Bean, R., Doré, O., et al. 2007, *ApJS*, **170**, 377
- Spruit, H. C. 1996, in *NATO ASI Ser., Ser. C*, ed. R. A. M. J. Wijers, M. B. Davies, & C. A. Tout, Vol. 477 (Dordrecht: Kluwer), 249
- Spruit, H. C., Stehle, R., & Papaloizou, J. C. B. 1995, *MNRAS*, **275**, 1223
- Steenbeck, M., Krause, F., & Rädler, K.-H. 1966, *ZNatA*, **21**, 369
- Stein, Y., Dettmar, R. J., Irwin, J., et al. 2019, *A&A*, **623**, A33
- Steinwandel, U. P., Beck, M. C., Arth, A., et al. 2019, *MNRAS*, **483**, 1008
- Steinwandel, U. P., Boess, L. M., Dolag, K., & Lesch, H. 2021, arXiv:2108.07822
- Steinwandel, U. P., Dolag, K., Lesch, H., et al. 2020a, *MNRAS*, **494**, 4393
- Steinwandel, U. P., Moster, B. P., Naab, T., Hu, C.-Y., & Walch, S. 2020b, *MNRAS*, **495**, 1035
- Su, K.-Y., Hayward, C. C., Hopkins, P. F., et al. 2018, *MNRAS*, **473**, L111
- Subramanian, K., & Barrow, J. D. 2002, *MNRAS*, **335**, L57
- Teklu, A. F., Remus, R.-S., Dolag, K., et al. 2015, *ApJ*, **812**, 29
- Toomre, A. 1981, in *Struct. Evol. Norm. Galaxies, Proc. Adv. Study Inst.*, ed. S. M. Fall & D. Lynden-Bell (Cambridge: Cambridge Univ. Press), 111
- Tüllmann, R., & Dettmar, R. J. 2000, *A&A*, **362**, 119
- Vargas, C. J., Walterbos, R. A. M., Rand, R. J., et al. 2019, *ApJ*, **881**, 26
- Vazza, F., Brunetti, G., Brügggen, M., & Bonafede, A. 2018, *MNRAS*, **474**, 1672
- Vazza, F., Dolag, K., Ryu, D., et al. 2011, *MNRAS*, **418**, 960
- Wardle, M., & Koenigl, A. 1993, *ApJ*, **410**, 218
- Weber, E. J., & Davis, L. J. 1967, *ApJ*, **148**, 217
- Whitaker, K. E., Franx, M., Leja, J., et al. 2014, *ApJ*, **795**, 104
- Wolfé, A. M., Jorgenson, R. A., Robishaw, T., Heiles, C., & Prochaska, J. X. 2008, *Natur*, **455**, 638
- Xu, S., & Lazarian, A. 2020, *ApJ*, **899**, 115
- Yusef-Zadeh, F., Roberts, D. A., Goss, W. M., Frail, D. A., & Green, A. J. 1996, *ApJL*, **466**, L25
- Zeldovich, Y. B. 1983, *Magnetic fields in astrophysics* (New York, NY: Gordon and Breach)
- Zjupa, J., & Springel, V. 2017, *MNRAS*, **466**, 1625